ABSTRACT

HEGARTY, MEGHAN S. Design of an Intelligent Compression Stocking for Reducing Ulcer Healing Time. (Under the direction of Dr. Edward Grant).

Venous leg ulcers remain a problem in the United States, costing the health care industry nearly $1 billion annually. A major portion of this spending is incurred as a result of prolonged healing time. Compression therapy is known to promote recovery. This technique may be improved by allowing for dynamic customization of treatment parameters. The design of a sensing system for an intelligent compression stocking is described in this thesis. This sensing system will eventually serve as a means by which to quantify the performance of the stocking through the continuous measurement of key physiological variables. Blood flow velocity will be measured using an acoustic array, and leg volume will be quantified using bio-impedance techniques. Preliminary experiments were conducted in order to verify the responsiveness and practicality of using these technologies to monitor ulcer healing. The Edema Monitoring System was capable of resolving small changes in leg volume resulting from artificially-induced swelling. Unfortunately, the Acoustic Blood Flow Measurement System did not perform acceptably in terms of accuracy and robustness. Future directions for this technology include finding a more acceptable means by which to measure blood flow velocity, improving the sensing system by incorporating additional optimization parameters, exploring the use of alternative actuation mechanisms, and expanding its use to encompass all medical-grade compression stockings.

Design of an Intelligent Compression Stocking for Reducing Ulcer Healing Time

by

Meghan Sarah Hegarty

A thesis submitted to the Graduate Faculty of
North Carolina State University
in partial fullfillment of the
requirements for the Degree of
Master of Science

Biomedical Engineering

Raleigh, North Carolina

2007

Approved By:

Dr. Brooke Steele	Dr. Carol Giuliani

Dr. Edward Grant
Chair of Advisory Committee

DEDICATION

To Mom, Dad, Anne, and Matthew...

BIOGRAPHY

Meghan S. Hegarty was born on September 25, 1983 in Boston, MA to parents Emily and John Hegarty. Meghan studied Biomedical Engineering at the University of Hartford, and received her B.S. in Engineering from this university in May, 2005. She then went on to North Carolina State University (UNC/NCSU Joint Department of Biomedical Engineering) to complete her graduate studies. Meghan received a National Science Foundation Graduate Student Fellowship in May, 2007. She is also a member of Tau Beta Pi.

ACKNOWLEDGMENTS

This material is based upon work supported under a National Science Foundation Graduate Research Fellowship. Any opinions, findings, conclusions or recommendations expressed in this publication are those of the author and do not necessarily reflect the views of the National Science Foundation.

I would first like to thank my family for encouraging me in every aspect of my life. Their guidance sparked an early interest in science and math, and ultimately helped me choose engineering as a career path. Furthermore, their love and patience has given me the strength to continue to excel at my academic studies.

I would also like to thank Dr. Edward Grant for accepting me into the Center for Robotics and Intelligent Machines and supporting me throughout my graduate studies. His enthusiasm and friendship are much appreciated. Additionally, I would like to acknowledge the other members of my committee, Dr. Carol Giuliani and Dr. Brooke Steele, for their assistance.

I am also grateful for our project sponsors at the Carolon Company. The concept for a dynamic, physiologically-controlled compression stockings originated at this company, and was brought to us at the Center for Robotics and Intelligent Machines in the winter of 2007. For over a year, the Carolon Company has been instrumental in supporting this research project. I would like to specifically thank Larry Reid for working closely with us throughout this project.

I also wish to express my appreciation for the assistance given to me by my colleagues at the Center for Robotics and Intelligent Machines. Carey Merritt and Matthew Craver provided valuable input into many aspects of this project. They were always there to answer my never-ending question related to hardware and software. I would also like to acknowledge and thank my partner in this project, Frederick Livingston. Additionally, I am grateful for the support provided by Kyle Luthy and Dr. Leonardo Mattos.

TABLE OF CONTENTS

LIST OF TABLES

LIST OF FIGURES

LIST OF ABBREVIATIONS

AC:	Alternating Current
A/D:	Analog-to-Digital
APG:	Air Plethysmography
CFR:	Capillary Filtration Rate
CMRR:	Common Mode Rejection Ratio
CW:	Continuous Wave
DC:	Direct Current
ECG:	Electrocardiogram
GUI:	Graphical User Interface
HCFA:	Health Care Financing Administration
IPC:	Intermittent Pneumatic Compression
IPG:	Impedance Plethysmography
LDF:	Laser Doppler Flowmetry
MRI:	Magnetic Resonance Imaging
NIR:	Near-Infrared
OCT:	Optical Coherence Tomography
ODT:	Optical Doppler Tomography
Op-Amp	Operational Amplifier
PC:	Personal Computer
PPG:	Photoelectric Plethysmography
RMS:	Root Mean Square
SPG:	Strain Gauge Plethysmography

Chapter 1

Introduction

The work reported on in this thesis represents a collaborative effort between the Center for Robotics and Intelligent Machines (North Carolina State University) and the Carolon Company (Rural Hall, NC). The Carolon Company is a leading US-based manufacturer of medical-grade compression hosiery.

1.1 Motivation

Between 500,000-600,000 persons living in the United States are suspected to be suffering from venous leg ulcers [1]. As the prevalence of leg ulcers is higher among older adults, this number is expected to rise as the U.S. population ages [2]. Treatment costs for this condition are substantial, with spending reaching upwards of $775 million to $1 billion annually [1]. Unfortunately, under current Health Care Financing Administration (HCFA) restrictions, the cost of care often times falls to the patient. Because many cannot afford this expensive treatment, patient compliance remains a major problem [1, 3].

A retrospective study conducted by Olin et al. set out to determine the source of out-patient expenses related to venous leg ulcer treatment. Home health care and hospitalization accounted for nearly 75% of the total cost incurred even though only a minority of patients received these services. A strong relationship between total cost and the “duration of active therapy, ulcer size, and the presence of at least one comorbidity” was also revealed [1]. Of these factors, the duration of active therapy can be most easily controlled; the other factors are related to the initial condition of the patient. Thus, in order to reduce patient costs, an inexpensive means of reducing treatment time must be developed.

Current treatment options for venous leg ulcers center around the use of compression therapy. Compression therapy is often delivered in the form of bandages or medical-grade stockings, although pneumatic compression devices are occasionally used. Of these three technologies, medical-grade stockings are the most appropriate for out-patient use (i.e. bandages must be applied by trained professionals and pneumatic compression requires the patient to remain seated for long periods of time). Although compression stockings can be custom-made, this adds considerable cost to the product. The majority of prescribed stockings are ready-made, allowing the physician to choose among different levels of compression. This minimizes the degree of patient individualization, and consequently, healing rate efficiency.

A potential solution to this problem involves the use of an intelligent system that can vary the pressure delivered based upon measured physiological variables [4]. The research reported on in this thesis describes the design of a ready-made compression stocking that can dynamically regulate the amount of pressure delivered in order to optimize therapy on an individual basis. Not only is this expected to reduce the time and cost of treatment, but will enable investigation of the effects of different pressure profiles [5].

1.2 Thesis Goals

The objectives of this thesis are to describe the:

- Technology currently available for venous leg ulcer treatment
- Basic design of an intelligent compression stocking
- Development and implementation of an acoustic array for sensing blood flow velocity
- Development and implementation of a bio-impedance measurement system for edema monitoring
- Future directions and applications for this technology

1.3 Thesis Outline

The design and development of an intelligent compression stocking are described in this thesis. An overview of the current technology available for the treatment of venous leg ulcers is discussed in Chapter 2. In addition to conventional treatment modalities (i.e. compression bandages and stockings), alternative treatment options are also examined. The design of a dynamically regulated compression stocking is presented in Chapter 3. A summary of the mechanical and sensing

systems is included. Chapter 4 contains a detailed explanation concerning the use of an acoustic array for the purposes of measuring blood flow velocity. An analysis of the system's ability to resolve arterial and venous blood flow is provided. Evidence to support the use of a bio-impedance analysis system for the purposes of monitoring edema is reviewed in Chapter 5. A detailed description of the system used is also presented. The final chapter contains a summary of all experimental findings, and outlines future directions and applications for this system.

Chapter 2

Literature Review

Venous leg ulcers result from incompetence of the valves connecting the superficial and deep veins [6]. Failure of these valves causes blood to flow from the deep to the superficial system, resulting in superficial venous hypertension [6, 7]. The skin capillaries cannot withstand this prolonged high pressure, and become insufficient. As a result, oxygen delivery to the tissue is decreased and leg ulcers develop [7]. Please refer to Figure 2.1 for clarification.

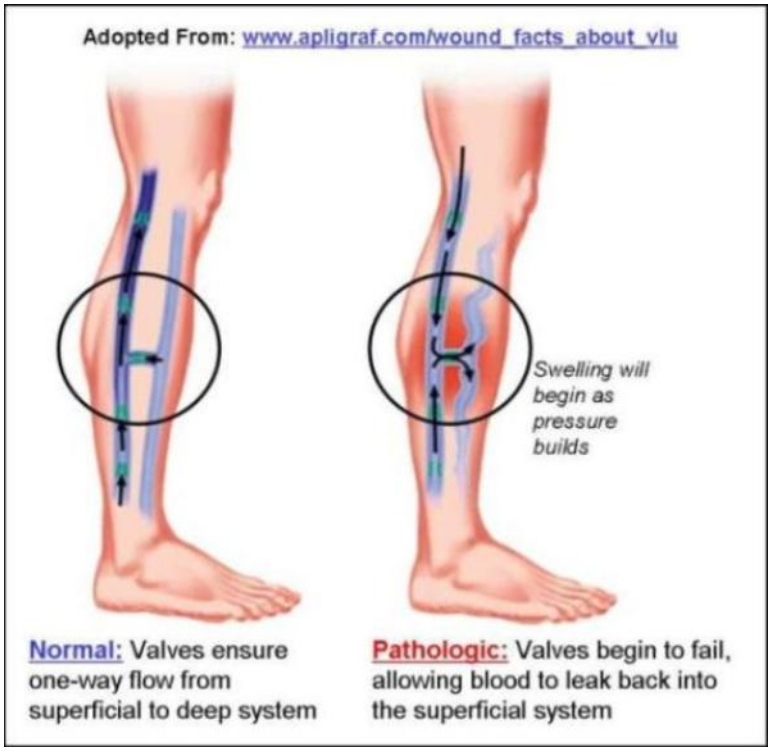

Figure 2.1: Superficial Venous Hypertension

Treatment of leg ulcers involves management of the underlying pathology, as well as the symptoms associated with the ulcer. Compression therapy is considered to be the cornerstone of this treatment process. Healing rates of 40-70% after three months of therapy, and 50-80% after six months of therapy have been reported [8].

The mechanism by which compression aids in ulcer healing is not completely understood. It has been hypothesized that "the application of external pressure to the calf muscle raises the interstitial pressure, decreases the superficial venous pressure, and improves venous return– leading to a reduction in the superficial venous hypertension" [6]. The filtration-diffusion equilibrium is thus restored, and leakage of solutes and fluids into the interstitial space is reduced [9, 10, 11]. The application of external pressure also serves to compress the superficial veins, preventing excessive venous distension [5, 10]. Because the cross-sectional area of the vessel is reduced, the velocity of venous blood flow is increased [5, 12]. Together, these factors together serve to reduce edema, which relieves pain resulting from excessive swelling and allows the ulcer to heal.

Compression is normally delivered by bandages (inelastic, elastic, and/or a multi-layer system) or by medical compression stockings [2, 6, 11]. For ulcers that do not respond well to bandages and/or compression stockings, pneumatic compression therapy may be appropriate [2, 6, 13, 14, 15]. Each of these compression modalities will be discussed in the following sections.

2.1 Compression Bandages

Compression bandages are classified based upon the amount of external pressure they provide (Class 1, Class 2, and Class 3) [6] and their extensibility (short stretch, medium stretch, and long stretch) [9]. The bandage's extensibility and the amount of pressure delivered are related by Laplace's Law (i.e. the pressure exerted by the compression bandage is directly proportional to the tension or extensibility of the bandage, and inversely proportional to the radius of the leg). For simplicity, we will limit our discussion to inelastic (short stretch) and elastic (long stretch) bandages.

Inelastic compression can be delivered by tight, short-stretch bandages and/or semi-rigid zinc plaster bandages (Unna's boots, DomePaste, UnnaFlex) [2, 9]. Inelastic compression achieves its effect by opposing the increase in muscle volume caused by a contraction [9, 11]. Because the muscle must contract, the greatest amount of pressure is supplied when the patient is active (approximately 40 mmHg during walking), but little to no compression is provided at rest (approximately 20 mmHg) [7, 9, 11]. Due to their low resting pressure, short stretch bandages do not need to be removed at night [11]. In fact, patients are able to tolerate wear of these bandages for multiple days

(normally 7-10 days) [9, 11]. Inelastic compression is therefore appropriate for patients who cannot fit their own bandages. Unfortunately, short stretch bandages have a tendency to lose a significant amount of their pressure within the first few hours of application, with more than half of their original pressure being lost over the entire wear cycle [9, 11].

Elastic compression utilizes the recoil force of the elastic fibers to provide compression during both exercise and rest. In the case of elastic compression, contraction of the muscle serves to enhance the amount of compression delivered at resting levels [7, 11]. Although the working pressure (i.e. the amount of compression provided during activity) is generally less than that provided by inelastic bandages, long stretch bandages are able to maintain a constant interface pressure over a longer wear period [9, 11]. Unfortunately, because pressure is constantly being applied, this form of therapy may not be well tolerated by inactive patients. Elastic bandages must also be removed at night to prevent complications with arterial reflux [7, 11].

Four-layer bandages combine aspects of inelastic and elastic compression into one system. Their mechanism of action is similar to that of short stretch bandages insofar as they do not provide significant compression when the patient is lying down [11]. Multilayer systems generally consist of an absorbent pad (i.e. orthopedic wool), crepe, a long-stretch bandage, and a medium-stretch cohesive outer wrap [2, 9, 11]. The orthopedic wool serves to absorb exudate and cushion bony prominences, which are naturally subject to higher levels of pressure. The crepe helps to hold the padding in place, while the long stretch bandages are used to provide compression. The outer cohesive bandage strengthens and supports the underlying system. This complex wrapping procedure allows four-layer bandages to secure permanent pressure, with only modest pressure loss over the entire wear cycle (normally 5-7 days) [11].

Both inelastic and elastic bandages have been shown to achieve ulcer healing rates of 40-70% at three months; there is no strong evidence to suggest that one form of bandaging is more effective than the other [9]. Because all compression bandages must be applied by properly trained staff, success is largely dependent on the skill of the therapist [9, 11]. Unfortunately, without some means of performance feedback, most therapists cannot precisely gauge the amount of pressure being applied [8, 9]. “An interface pressure of approximately 40 mmHg measured at the medial gaiter area is generally agreed to be a safe and effective target level of compression therapy” [9]. If the bandages are wrapped too loosely, efficient edema reduction may not be achieved. Bandages that are wrapped too tightly may dangerously reduce blood flow to the leg (i.e. interface pressure exceeding 60 mmHg have been shown to produce an 84% decrease in blood flow) [5, 6, 9]. Long stretch elastic bandages are generally considered to be easier to use than short stretch inelastic

bandages, rendering them more appropriate for use with less-experienced staff [11]. Safe levels of compression can, however, be attained with either form of bandaging provided that sufficient training and performance feedback is available [9].

2.2 Compression Stockings

Compression stockings achieve effects similar to long-stretch elastic bandages, applying compression to the leg both during activity and at rest. The stockings are knitted so that pressure is applied in a graduated (versus uniform) manner, with the greatest amount of pressure being applied at the ankle. Although the level of compression delivered can vary between different classes of stockings, an ankle-to-popliteal ratio of 18:8 mmHg is generally adhered to; gradient compression at this intensity was previously found to elicit the greatest increase in femoral vein flow velocity [16].

Factors such as the level of pressure delivered, the stiffness of the material, the type of knit, and length of the stocking can vary between stocking types. Compression stockings are generally classified by the level of compression delivered. For uniformity, all compression measurements are specified at the ankle level, although measurement techniques and class definitions differ between countries (see Table 2.1).

Table 2.1: U.S. and European Compression Stocking Class Definitions

Class	**Pressure (mmHg)**		**Clinical Uses**
	U.S.	**British**	
I	20-30	15-21	Minor varicose veins, functional venous insufficiency, mild edema
II	30-40	23-32	Slight chronic venous insufficiency, mild/moderate edema, surgery
III	40-50	34-46	Advanced chronic venous insufficiency, leg ulcers, severe edema
IV	$>$50	$>$49	Very severe chronic venous insufficiency, very severe edema

**Table adopted from* [11, 3]

Because leg ulcers generally require high levels of compression to achieve efficient healing, U.S. Class II and III stockings and European Class III and IV stockings are generally used. Unfortunately, higher level compression stockings are stiffer and harder to put on, which may pose a problem for elderly and/or arthritic patients. In these cases, lower level stockings can be layered in order to achieve the desired effect [2, 11, 3].

The stiffness of the compression stocking also affects venous ulcer healing rates [17]. The stiffness of the stocking refers to the elasticity or slope value of the material. "The slope value is defined as the increase in pressure (mmHg) of the stocking when the circumference of the stocking increases by 1 cm, expressed as kPa/cm^2" [17]. Stockings within the same compression class can

have different slope values. Stiffer stockings (i.e. higher slope value) are able to achieve higher pressures during muscle activity than less stiff stockings (i.e. lower slope value). Van Geest et al. compared the effect of three different compression stockings on capillary filtration rate (CFR; used as an indicator of ulcer healing)– Type 1: low slope, 30 mmHg; Type 2: high slope, 30 mmHg; and Type 3: low slope, 34.5 mmHg [17]. The results of this study indicate a significant improvement in CFR when compression versus no compression was used, with Type 2 and Type 3 stockings showing statistically greater improvement over Type 1 stockings [17]. This points to a need for physicians to take into account the slope value of the material when prescribing compression stockings, as severe/recurrent edema may merit the use of a stiffer product [7, 17].

The type of knit used can also vary between compression stockings. Double-faced, flat bed-knitted stockings (with a seam) are made from elastic inlaid thread (i.e. “elastic thread that does not form stitches or loops and is inlaid in the direction of the course”) and/or knitted elastic threads [7]. These flat-knitted stockings are formed by varying the number of needles used in the knitting process. Because the number of stitches can change between rows, the same level of compression can be achieved in stockings of different circumference. As a result, flat-knitted stockings can be custom-made to a precision of 0.5 cm [7]. Single-faced, circular knit stockings (seamless) are also made from elastic inlaid and/or knitted elastic threads. These round-knitted stockings are formed by adjusting the “tightness of courses and the tension of the knitted threads” [7]. Consequently, stockings with different circumferences are characterized by different levels of tension, rendering flat-knit stockings of limited use for non-confection legs (i.e. from edema). Double- or single-faced stockings do not use elastic inlaid threads; the method of knitting is identical to those previously described. Because elastic inlaid threads are needed to achieve higher compression levels, double- or single-faced stockings are usually reserved for lower compression classes [3, 7].

Compression stockings suffer from many of the same drawbacks as elastic bandages. Improperly fit stockings can result in inefficient edema reduction if too loose, or necrosis and pressure damage if too tight. In order to avoid such dangers, leg measurements should be taken at regular intervals (i.e. an increase of 5 cm can double the amount of pressure) [5]. Compression stockings may be preferable to compression bandages insofar as they do not require a trained professional for application and removal. Additionally, compression stockings are able to maintain consistent levels of pressure for longer periods of time compared to compression bandages (normally 4 months for round-knitted stockings and 6-12 months for flat-knitted stockings) [7, 8].

2.3 Intermittent Pneumatic Compression (IPC)

Intermittent pneumatic compression (IPC) may be appropriate for ulcers that do not respond well to conventional therapy, and may be the only option available for patients who cannot tolerate wear of bandages or stockings due to skin allergies [2, 3, 6, 13, 14, 15]. This form of therapy may also be appropriate for non-compliant patients, as it requires significantly less wear-time compared to compression bandages and/or stockings.

An IPC device consists of an air pump that periodically inflates or deflates a bladder surrounding the leg. This bladder can be secured to the leg using a zipper stocking (U.S. Patent 5,814,003) or incorporated into a boot-like device [6]. A single bladder can be used to deliver uniform, pulsed compression, or multiple bladders can be used to deliver variable, graded compression [13]. Pressures ranging from 30-70 mmHg can be achieved with these systems [6]. Factors such as the type of compression cycle and inflation/deflation time can be customized to meet individual needs [13].

Studies undertaken to validate the use of IPC for ulcer healing have produced mixed results. When used in place of compression bandages and/or stockings, no significant difference was found between IPC and other techniques in terms of ulcer healing rate and edema reduction [13, 14]. This seems to indicate that IPC is comparable to compression bandages/stockings, and can be used in place of these treatments without compromising the health of the patient. Other studies have compared the use of IPC versus no IPC with compression stockings/bandages. Two such studies found a significant improvement in healing time when IPC was used with traditional compression therapy, while another study reported no difference in healing time [13, 15]. Of note is the fact that a sequential compression regimen (i.e. multiple bladder systems) was used in the two studies that reported a significant difference in healing rate, while a uniform compression regimen (i.e. single bladder system) was used in the study in which no significant difference was reported. This finding agrees with previous evidence supporting the use of graduated compression versus uniform compression [16].

2.4 Other Systems

Asada et al. have been working to create a closed-loop IPC system [4]. The Real Pro massage chair (Matsushita Electric Works, Ltd.) is used to apply sinusoidal compression to the ankle and calf. Bio-impedance, heart rate, oxygen saturation, and temperature sensors are used to provide relevant physiological information to the system. The bio-impedance sensors detect changes

in lower leg volume resulting from fluid accumulation and venous pooling (i.e. impedance and volume are inversely related). A modified Quantum X bio-impedance analysis system (RJL Systems) is used to provide continuous impedance information. Heart rate and oxygen saturation are measured using the Nellcor N-395; these variables are presumably used to tune the system. The temperature of the foot is measured using a simple thermistor. Skin temperature is related to the degree of vasoconstriction/vasodilatation of the blood vessels, which ultimately affects the degree of blood flow in the leg.

This physiological data serves as an input to the Bi-Compartmental Model, which is used to control the massage chair. The Bi-Compartmental Model is a simplified version of the Human Observer Model developed by Asada et al. [4]. The Bi-Compartmental Model divides the body into two major compartments- the upper (head, upper extremities, and torso) and the lower (legs). By analyzing the lower compartment only, one can extract information concerning circulation in the legs. This information can be used to detect the effect of postural changes on blood flow and circulatory changes on interstitial fluid accumulation. In order to reflect changes in the degree of edema formation, interstitial fluid accumulation must be isolated from venous blood volume.

A simple experiment was conducted in order to confirm the system's ability to track and alleviate the symptoms associated with edema formation. This experiment revealed that the model could accurately calculate changes in interstitial fluid accumulation when properly tuned. In order to tune the model, blood pressure information was used. Venous pooling could also be detected, and was well correlated with changes in posture. Additionally, interstitial volume was found to decrease over the course of the therapy session. In order to further improve the system, Asada et al. recommended collecting a broader range of physiological data (i.e. EMG, blood pressure, etc.). Unfortunately, adding more parameters serves to further complicate the Bi-Compartmental Model used to control the system [4].

2.5 Summary

A careful review of literature has revealed a variety of technologies available for compression therapy. Compression stockings and bandages can be used to continuously apply pressure during activity and/or rest. While appropriate for continuous wear applications, they do not offer a simple means by which to continuously alter the amount of pressure being applied. IPC devices allow for some degree of control over the pressure regimen, and may be appropriate for patients who do not respond well to conventional therapy with bandages and/or stockings. Preliminary work

by Asada et al. has explored the use of physiological monitoring in conjunction with an IPC device. Unfortunately, these systems are not portable and require the patient to remain seated during use. To date, no previous work in the area of a portable, intelligently-controlled compression stocking has been reported.

Chapter 3

Compression Stocking Design

A dynamically controlled, ready-made compression stocking would allow for individualized treatment at a reduced cost compared to custom-made stockings. This could translate into accelerated ulcer healing, which is beneficial both in terms of the patient's well-being and expense. Dynamic control can be accomplished by continuously monitoring key physiological variables using durable, non-invasive, low-profile sensors. An intelligent control algorithm can then be used to increase or decrease the amount of pressure delivered by the stocking. By tracking changes over time, the efficiency of the stocking can be judged.

3.1 Stocking Mechanics

The proposed stocking consists of three modules– a low-compression under-stocking, a variable compression over-stocking, and a sensing system (see Section 3.2). The low-compression under-stocking will deliver pressure according to the standards specified for the lowest-grade compression stocking. This will provide a starting point for all patients in order to limit the extent to which the system has to work to change pressure. The under-stocking will be easy to put on so as not to pose a problem for elderly and arthritic patients.

Variable pressure delivery will be controlled pneumatically. Air will be pumped into the system using miniature diaphragm pumps (T2-03 or T2-05, Parker Hannifan Corporation– Pnuetronics Division). Miniature pumps can precisely deliver small volumes of air over long periods of time. These pumps are generally lightweight, unobtrusive, and quiet.

Engineers at the Carolon Company are currently investigating the possibility of knitting miniature silicon tubes into the compression stocking. Tubing as small as 0.065" OD (approximately

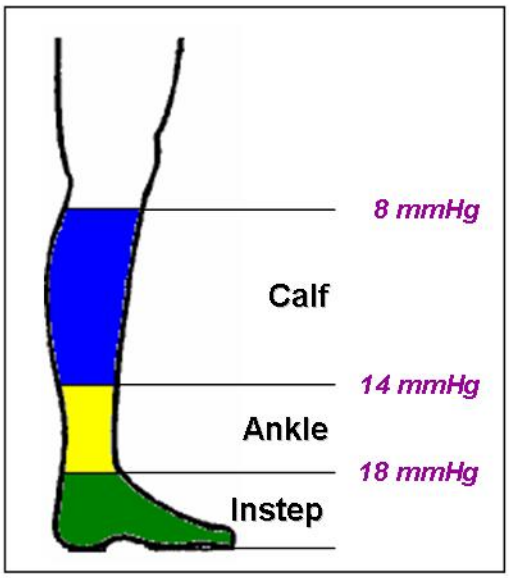

Figure 3.1: Compression Stocking Zones and Pressure Profile

1.65 mm) is available (2810304, New Age Industries). Groups of tubes will share a common inlet and exhaust valve. Sectioning will be based the zones currently used in compression stockings to achieve a gradient pressure profile(see Figure 3.1).

Because each zone is separately controlled, the use of different pressure profiles can be explored (i.e. there is no strong evidence to support the use of currently adhered to standards for different vascular pathologies) [5]. Additionally, it may also be beneficial to isolate areas of markedly different circumference. At least one study found a significant variation in the pressure delivered at different sites around the ankle. The lowest pressure was reported at a medial site located just above the ankle, which is the area most susceptible to ulcer formation [18]. By isolating certain key areas, a more uniform pressure profile can be achieved. This should serve to decrease ulcer healing time and prevent recurrence.

Two designs have been proposed related to the use of three discrete stocking modules; the sensing system is kept separate from the mechanical system in both. In the first design, two stockings will be used– a fixed compression under-stocking and a variable compression over-stocking. The stockings will be layered and snapped together in order to achieve the desired effect. This design is advantageous insofar as it allows for variable regulation of all three stocking zones and provides easy replacement options (i.e. both stockings can be replaced separately as needed). Additionally, patients who already own stockings can purchase the variable compression over-stocking and sensing system in order to transform their ordinary stockings into an intelligent system. Disad-

vantages include confusion over the order in which the stockings should be layered. In the second design, the variable-compression over-stocking will fold over the under-stocking, similar to a soccer sock. The over-stocking will then snap down over the under-stocking below the ankle level. This design is advantageous insofar as it prevents one of the stockings from being lost and may be less expensive to manufacture (i.e. less material). Disadvantages include variable regulation of only two zones (i.e. the ankle and calf) and the need to replace the whole system at once. Additionally, because this stocking cannot be used with already existing product, initial market acceptance may be lower.

3.2 Sensing System

Continuous-wear systems require the use of portable, non-invasive, robust components. Portability can be achieved by using lightweight sensors and keeping the overall part-count low. Whenever possible, low-profile sensors should be selected in order to increase user comfort. This also serves to increase durability, as low-profile components are less likely to incur incidental damage. Additionally, as the users of this device are expected to be ambulatory, the sensing system must be able to tolerate movement artifacts without loss of resolution. User safety must also be taken into account because some technologies could introduce unacceptably high levels of radiation, etc. into the body if used for an extended period of time. All of these factors must be considered when choosing an appropriate sensing system for use with the pneumatic compression stocking previously described.

3.2.1 Blood Flow Velocity

Appropriate blood flow/velocity is needed for efficient ulcer healing. Blood flow and velocity are directly related by the equation:

$$Q = V * A$$

where Q is blood flow, V is velocity, and A is the cross-sectional area of the vessel. Arterial flow/velocity is an indicator or nutrient and oxygen delivery to the ulcer site. Venous flow/velocity is and indicator of waste removal. Additionally, low venous velocity is associated with an increased risk for dangerous clot formation.

For this application, the velocity of blood flow is of greater concern because it directly relates to the hypothesized effect of compression on venous return (see Chapter 2). If the cross-

Table 3.1: Technologies for Measuring Blood Flow

Type	**Implementation**	**Applications**
Auscultation	Turbulent (i.e. arterial) blood flow can be heard using a stethoscope. Continuous flow recordings can be made using a microphone or piezoelectric crystal [19, 20].	Listening to arterial blood flow for the purposes of assessing circulatory health
Doppler Ultrasound	Piezoelectric crystals generate a sound beam. Moving blood causes a frequency shift in the reflected wave, which is linearly related to velocity. Continuous wave (CW) systems use two piezoelectric crystals- one for transmitting and one for receiving. Pulsed systems use only one crystal, which serves as both a transmitter and receiver [21].	Measuring peak arterial and venous blood flow velocity [21]
Phase-contrast, gradient-echo MRI	Two sets of MRI data with "pulse sequences that have a different gradient first moment in the direction of interest" are used to detect a phase shift in transverse magnetism, which is proportional to flow velocity [22].	Measuring average arterial and venous blood flow [22]
NIR Spectroscopy	Photodetectors are used to measure differences in the absorption of NIR and red light by the tissue. Venous blood flow is proportional to the change in deoxyhemoglobin concentration. Arterial blood flow can be calculated by subtracting changes in the deoxyhemoglobin concentration from the total hemoglobin concentration [12].	Detecting changes in blood flow and measuring tissue oxygenation [12]
Optical Doppler Tomography (ODT)	ODT combines conventional laser Doppler flowmetry (LDF) with optical coherence tomography (OCT) to produce high-resolution sectional images. A NIR superluminescent diode serves as the light source, and a photodetector is used to measure the optical interference-fringe intensity. Flow velocity is related to the frequency shift that occurs when "light backscattered from a moving particle interferes with the reference beam" [23].	High resolution imaging of microcirculation and tissues surrounding the vessel [23]

sectional area of the vessel can be continuously measured, either blood flow or velocity information can be used. Auscultation techniques, ultrasound, magnetic resonance imaging (MRI), and near-infrared (NIR) monitoring have all been used to assess blood flow. The implementation of these techniques are presented in Table 3.1.

Of these technologies, MRI is not appropriate for continuous wear applications because it is not portable. NIR techniques can also be eliminated because they are highly susceptible to movement artifact, with any change in the optical pathway serving to distort the measurement. This leaves ultrasound as the only proven method for measuring both arterial and venous blood flow velocity. It is interesting to note, however, that ultrasound technicians often confirm arterial or venous flow by by listening to the flow profile. This leads to the possibility of using a highly sensitive microphone (i.e. modified auscultation unit) to listen for arterial and venous flow. Peaks in the corresponding profiles could be tracked down the length of the vessel, and the time delay introduced between measurement points used to calculate blood flow velocity. This technique may offer a low-cost alternative to ultrasound, and will be discussed further in Chapter 4.

3.2.2 Edema Monitoring

Edema reduction is also closely coupled to ulcer healing. Edema is caused by an abnormal increase in the interstital fluid volume of any tissue, which causes the tissue to swell. The degree of edema can be monitored by tracking changes in leg volume over time. Changes in leg volume are conventionally measured using plethysmographic techniques. There are four major types of plethysmography– (1) air, (2) impedance, (3) photoelectric, and (4) strain gauge [24]. The implementation of these techniques are presented in Table 3.2.

Table 3.2: Types of Plethysmography

Type	**Implementation**	**Applications**
Air (APG)	An air-filled cuff is used to measure the rate of change of volume, which corresponds to changes in blood volume.	Clinical diagnosis and quantitative assessment of chronic venous insufficiency
Impedance (IPG)	A high frequency alternating current (AC) applied through electrodes is used to measure changes in electrical impedance, which corresponds to changes in blood volume.	Detection of blood flow disorders (i.e. arterial occlusive diseases and deep venous thrombosis)
Photoelectric (PPG)	A photodector is used to measure the intensity of reflected NIR and red light, which demonstrates changes in blood perfusion.	Detection of peripheral vascular disease and monitoring oxygen saturation
Strain Gauge (SPG)	A fine rubber tube filled with mercury is used to measure changes in limb circumference, which correspond to changes in blood volume.	Evaluation of acute/chronic venous insufficiency, evaluation of peripheral vascular disease, and detection of deep venous thrombosis

**Table adopted from* [24]

Of these four techniques, photoelectric plethysmography (also known as photoplethysmography or PPG) can be eliminated because it is more concerned with measuring changes in arterial blood flow than total limb volume. Air plethysmography (APG) can also be eliminated because it requires the use of a known, constant volume of air for measurement purposes. Additionally, the equipment required is cumbersome and not appropriate for use outside of the research laboratory [25]. This leaves impedance plethysmography (also known as bio-impedance or IPG) and strain gauge plethysmography (SPG) as viable options. Of these two, SPG may be simpler to implement (i.e. less components), but will presumably be more susceptible to movement artifact and sensor location. As the users of this device are expected to be ambulatory, this may present a problem. Additionally, most ready-made strain gauges require an estimate of the limb circumference for sizing purposes. If the size of the limb changes significantly, the accuracy of the sensor may suffer. Attaching the strain gauge directly to the stocking would also be unacceptable, as changes in compression level would alter the tension level of the material. Edema monitoring will therefore be implemented using bio-impedance analysis; this will be discussed further in Chapter 5.

Chapter 4

Use of an Acoustic Array for Measuring Blood Flow Velocity

The velocity of blood flow was identified as a key variable of interest (see Section 3.2.1). Briefly, arterial flow velocity serves as an indicator of nutrient and oxygen delivery to the wound site. Venous flow velocity can be used to gauge the rate of waste removal. Additionally, the chance for dangerous clot formation increases as venous velocity decreases.

Auscultation is a widely accepted technique for determining the quality of arterial blood flow. Beginning in the 1970's, highly sensitive microphones were used to continuously listen to and record arterial flow [19]. Peaks in the sound recording were well correlated with peaks in the arterial pressure waveform. In 1980, Wintermantel showed that differences in blood flow across a suture line could be resolved using two microphones (i.e. a diplo-microphone) [19].

Building on Wintermantel's work, an array of microphones can be affixed to a compression stocking for the purposes of sensing the arterial and venous pressure waveforms. These microphones will be located at known intervals along the course of the vessel, allowing blood velocity to be determined by calculating the time delay between waveform peaks. The peak of the arterial pressure waveform is associated with the rapid ejection of blood during ventricular systole. As the velocity of blood flow decreases, the pressure waveform decays and returns to the baseline (i.e. ventricular diastole). The arterial pressure waveform can thus be described as a periodic signal, with a frequency equivalent to the person's heart rate (see Figure 4.1). The peak of the venous pressure waveform is associated with expiration (i.e. during expiration, abdominal pressure falls and allows blood to return to the heart) [26]. During inspiration, abdominal pressure rises and impedes venous

return (i.e. the pressure waveform reaches a minimum) [26]. The venous pressure waveform can thus be described as a periodic signal, with a frequency equivalent to the person's respiratory rate (see Figure 4.1).

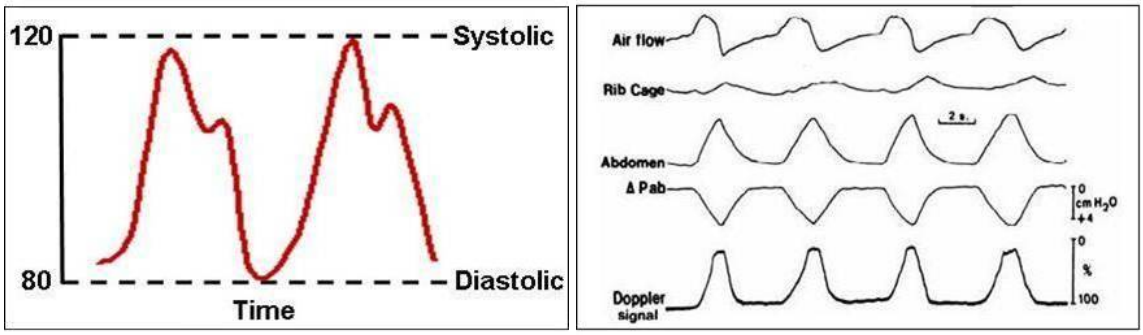

(a) Arterial Pressure Waveform (b) Venous Pressure Waveform [26]

Figure 4.1: Pressure Waveforms

4.1 Circuit Design

All components used in the Acoustic Blood Flow Monitoring System were originally selected to be low-power, low-noise, and low-cost. An effort was also made to minimize the footprint of the circuit, with much of the data processing and analysis being reserved for software. Please refer to Figure 4.2 for a general system layout and Appendix A for a complete circuit schematic.

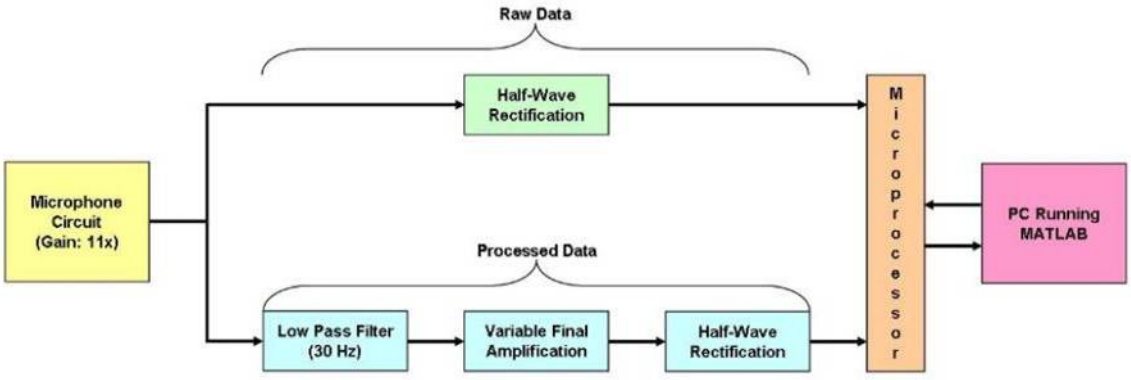

Figure 4.2: Acoustic Blood Flow Monitoring System

The pressure waveform is sensed by an electret condenser microphone (WM-52BM, Panasonic). An initial amplification of 11x is applied to the incoming signal to raise it above the noise floor

of the circuit. At this point, the signal is split so as to preserve the raw signal in the case of future hardware changes. The signal is then low-pass filtered (2^{nd} order Butterworth filter, cutoff: 30 Hz) to remove any high frequency noise. As the depth and size of the blood vessel are expected to affect signal strength, an adjustable, final stage amplification is applied to account individual differences. In order to avoid damaging the microprocessor (MSP430F149, Texas Instruments), negative signal components are eliminated through half-wave rectification. Negative signal components reflect rebounding of the microphone bladder after a step impulse, and are not related to the pressure waveform. Both the rectified raw signal and rectified processed signal are fed to the microprocessor, which communicates serially with a PC. Further processing and analysis are carried out using MATLAB.

A linear phase, 513-tap Parks-McClellan bandpass filter is used for arterial waveform filtering. The simulated frequency response of this filter is shown in Figure 4.3. This filter successfully removes movement artifacts resulting from breathing (i.e. the average adult respiratory rate is approximately 0.2-0.3 Hz) and any remaining high frequency noise while preserving important signal information (i.e. the average adult heart rate is approximately 1-1.5 Hz). Please refer to the supplemental CD for a copy of the MATLAB code used.

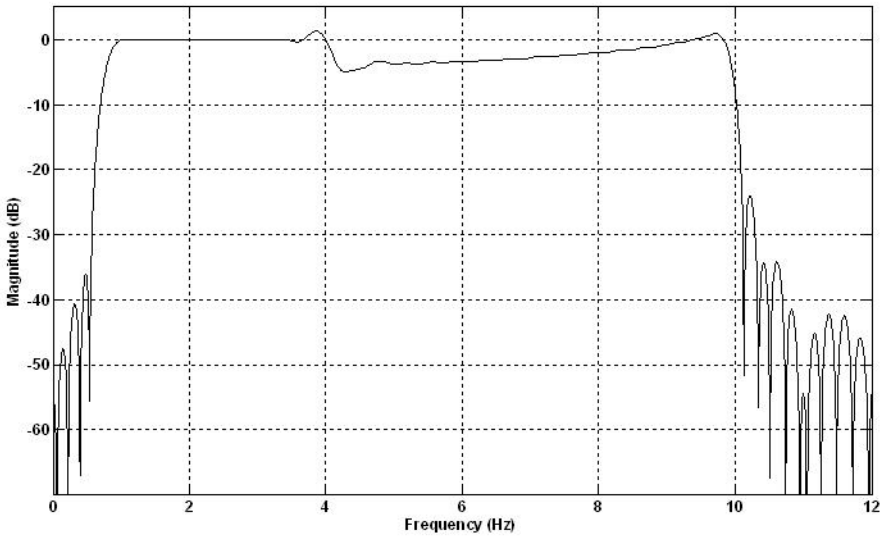

Figure 4.3: Frequency Response of the Digital Arterial Filter

A linear phase, 513-tap Parks-McClellan low-pass filter is used for venous waveform filtering. The simulated frequency response of this filter is shown in Figure 4.4. This filter successfully removes any high frequency noise and attenuates the arterial pressure wave signal (i.e. the femoral

artery and vein cross in some instances [27, 28]), while preserving important signal information. Please refer to the supplemental CD for a copy of the MATLAB code used.

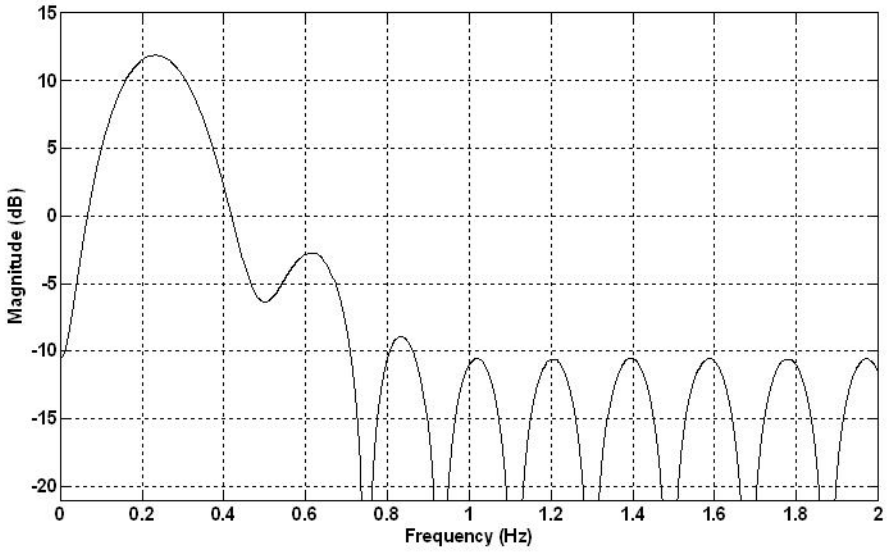

Figure 4.4: Frequency Response of the Digital Venous Filter

4.2 Experiments

Two experiments were conducted in order to test system accuracy (Section 4.2.1) and robustness (Section 4.2.2). In order to facilitate the measurement process (i.e. accessibility, subject comfort, etc.), pressure waveforms were collected from the radial artery and the median cubital vein. These vessels were also easier for untrained persons to locate.

The radial artery and femoral artery differ in terms of depth and size. The femoral artery is located significantly deeper than the radial artery (17 mm [29] versus 3.3 mm [30]). The depth of the artery directly affects the strength of the signal because the skin and subcutaneous tissue serve to dampen the sensed pressure waveform. This presumably means that the signal would need to be amplified to a greater extent when sensing the femoral versus radial artery pressure waveform. On the other hand, the average diameter of the femoral artery (8.5-8.75 mm [31]) is significantly larger than the radial artery (2.45 mm [31]). If both were located at the same depth, a larger signal may be sensed at the femoral artery because it would occupy a larger percentage of the microphone surface.

The median cubital vein and femoral vein also differ in terms of depth. The median cubital vein is classified as a superficial vein, and is much closer to the surface than the femoral vein (i.e.

a deep vein). Again, this presumably means that the sensed pressure waveform would be stronger at the medial cubital vein versus the femoral vein. Additionally, the wall thickness of lower extremity veins is usually greater than upper extremity veins due to increased hydrostatic pressure from gravity effects [32]. Thicker walls also serve to dampen and attenuate the pressure waveform. It is difficult to draw a direct comparison between the size of the median cubital and femoral veins because their elastic nature allows them to expand to accommodate increased blood volume [4]. Presumably, the femoral vein would be larger than the median cubital vein, as gravity effects would result in more venous pooling in the lower versus upper extremities.

4.2.1 Experiment 1– Measuring Arterial and Venous Pressure Waveforms

Purpose

The purpose of this experiment is to verify that the Acoustic Blood Flow Monitoring System can acceptably measure changes in arterial and venous blood flow.

Outline

Arterial and venous blood flow will first be measured under resting conditions. A blood pressure cuff will then be inflated to completely occlude blood flow (i.e. a maximum pressure of 160 mmHg will be used for arterial testing and a maximum pressure of 100 mmHg will be used for venous testing). A measurement will then be taken under known zero flow conditions. The cuff will then be deflated in 20 mmHg increments, and arterial and venous blood flow measured. When the applied pressure is greater than the subject's systolic pressure, both arterial and venous blood flow should be completely occluded. When the applied pressure falls below the systolic pressure, arterial flow is permitted, but venous flow remains stopped. When the applied pressure falls below 40-50 mmHg, venous flow should begin to return. A final resting measurement will be made in order to ensure that the microphone array did not become compromised during the course of the experiment.

The RMS voltage (i.e. indicator of signal power) will be computed at each step of the serial deflation. Under zero flow conditions, signal strength is expected to approximate that of ambient noise. Under full flow conditions, there should be a dramatic increase in signal power. This information will be used to determine if the Acoustic Blood Flow Monitoring System can acceptably detect both arterial and venous blood flow.

Methods

The subject's blood pressure and heart rate were measured using an automatic blood pressure monitor (OMRON IntelliSense Digital Wrist Blood Pressure Monitor, Model: HEM-609ECK). The cuff was then removed and the subject was asked to rest their right arm on a table with their palm facing up. A manual blood pressure cuff was placed around the subject's upper arm (the cuff was not inflated).

The experiment was divided into two tests– measurement of arterial blood flow and measurement of venous blood flow. The order in which these tests were conducted was randomly assigned, and subjects were given a 5 min rest between each test in order to ensure that blood flow had returned to normal. The experiment was immediately suspended if the subject experienced discomfort at any point during the test. At the conclusion of each test, the microphone was removed from the subject's arm and an ambient noise recording was made.

For arterial testing, the radial artery was palpated, and a mark was made to denote its location. The microphone was then attached to the subject's arm (i.e. against bare skin) using a Velcro strap so that the center of the microphone was aligned with the mark denoting the location of the radial artery. The fit of the strap was adjusted to minimize the application of external pressure. The resting arterial pressure pulse was recorded (i.e. no cuff inflation) for approximately 20 sec using the Acoustic Blood Flow Monitoring System (100 Hz sampling rate; final gain: 4.9x). MATLAB was used for data processing, storage, and display purposes. The blood pressure cuff was then inflated to 160 mmHg, and another measurement was taken. The cuff was deflated in 20 mmHg increments until it was again completely deflated (i.e. 0 mmHg), and measurements made. Each measurement was saved in a separate file.

For venous testing, the microphone was placed over the median cubital vein (at the elbow). The location of the vein was visually confirmed. The resting venous pressure waveform was recorded in the same manner as previously described (i.e. with the exception that a final amplification of 11x was used). The blood pressure cuff was then inflated to 100 mmHg, and another measurement taken. The cuff was deflated in 20 mmHg increments until it was again completely deflated (i.e. 0 mmHg), and measurements made. Again, each measurement was saved in a separate file.

Data Analysis

The RMS voltage of the signal was calculated at each pressure level. These values were normalized against the RMS voltage of the ambient noise. The normalized RMS voltages for each

subject were plotted against the applied pressure level (note: data was further normalized against the largest measured RMS voltage for each subject for graphical display purposes).

The time of signal appearance and disappearance was noted for each subject. For arterial testing, these values were compared to the subject's systolic blood pressure. For venous testing, these values were compared to pressures known to completely occlude venous blood flow (i.e. $>$50 mmHg). Fourier analysis of the raw data was carried out to assess where the strength of the signal lay.

Results

The Acoustic Blood Flow Monitoring System serves as an accurate indicator of arterial blood flow. Sample full flow (i.e. 0 mmHg applied pressure– starting measurement) and zero flow (i.e. 160 mmHg applied pressure) pressure waveforms for Subject 1 are shown in Figure 4.5. In all but one case (i.e. Subject 5), the appearance of a strong pulse signal occurred at the first instance when the applied pressure dropped below systolic pressure (see Table 4.1). For Subject 5, the pulse signal appeared one pressure step later than the recorded systolic pressure (i.e. the automatic blood pressure cuff indicated a systolic pressure of 121 mmHg for this subject, yet the pulse signal did not appear until the applied pressure fell to 100 mmHg). This is not seen as problematic because the recorded pressure of 121 mmHg falls near the borderline of the experimental pressure intervals. Additionally, there is a $\pm$3 mmHg error associated with the automatic blood pressure cuff, so the subject's true blood pressure may be below 120 mmHg, as determined experimentally.

Table 4.1: Appearance of Arterial Pulse Signal with Applied Pressure

Subject (SBP/DBP)	**Applied Pressure (mmHg)**									
	Start 0	**160**	**140**	**120**	**100**	**80**	**60**	**40**	**20**	**Stop** 0
1 (100/60)	S	N	N	N	N	S	S	S	S	S
2 (110/66)	S	N	N	W	S	S	S	S	S	S
3 (112/70)	S	N	N	N	S	S	S	S	S	S
4 (124/80)	S	N	N	S	S	S	S	S	S	S
5 (121/67)	S	N	N	N	S	S	S	S	S	S

* *S = strong pulse signal, W = weak pulse signal, N = no pulse signal*

When signal power (i.e. measured as RMS voltage) is plotted against applied pressure, one can see a clear trend in the data (see Figure 4.6 and Figure 4.7). When zero flow conditions are achieved, signal power drops dramatically. This is to be expected, as only noise is being measured. When systolic pressure is reached, there is a marked increase in signal power due to the appearance

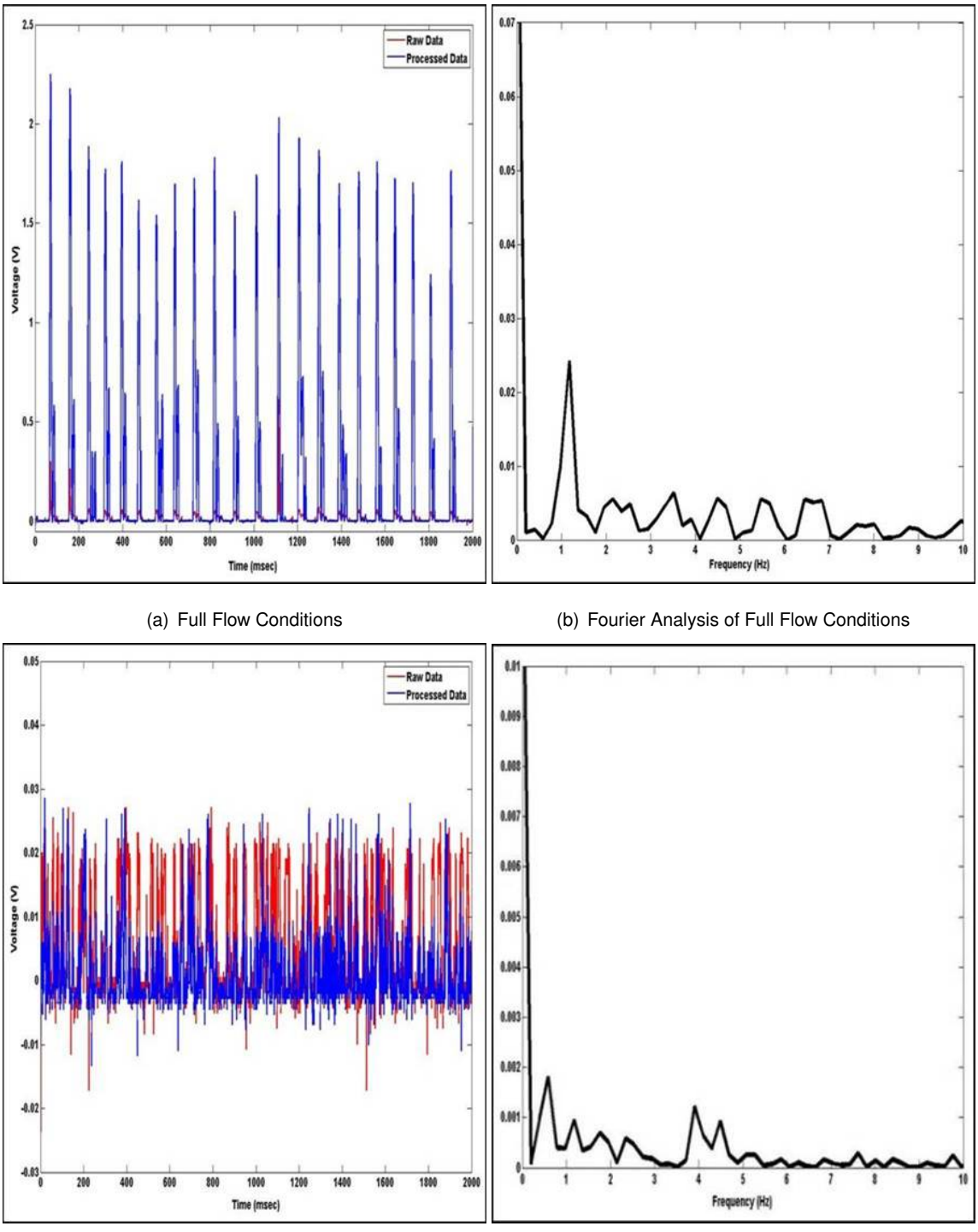

(a) Full Flow Conditions

(b) Fourier Analysis of Full Flow Conditions

(c) Zero Flow Conditions

(d) Fourier Analysis of Zero Flow Conditions

Figure 4.5: Influence of Applied Pressure on the Arterial Pressure Waveform– Raw Data

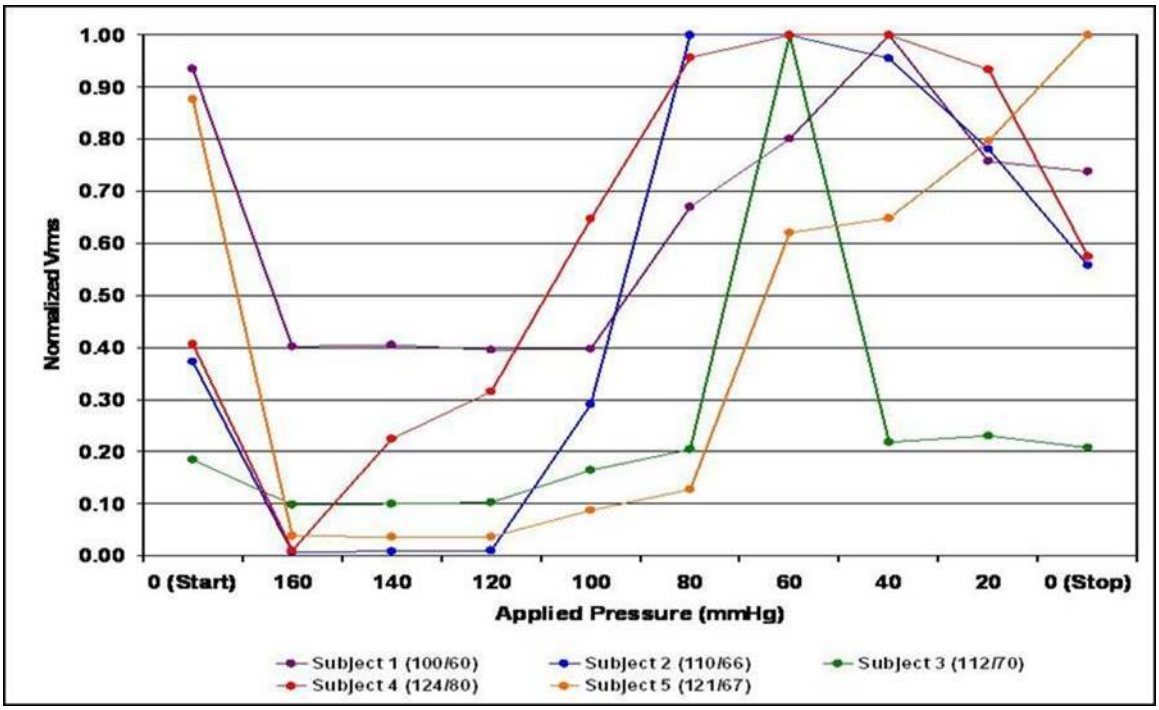

Figure 4.6: Normalized RMS Voltage vs. Applied Pressure– Arterial Raw Data

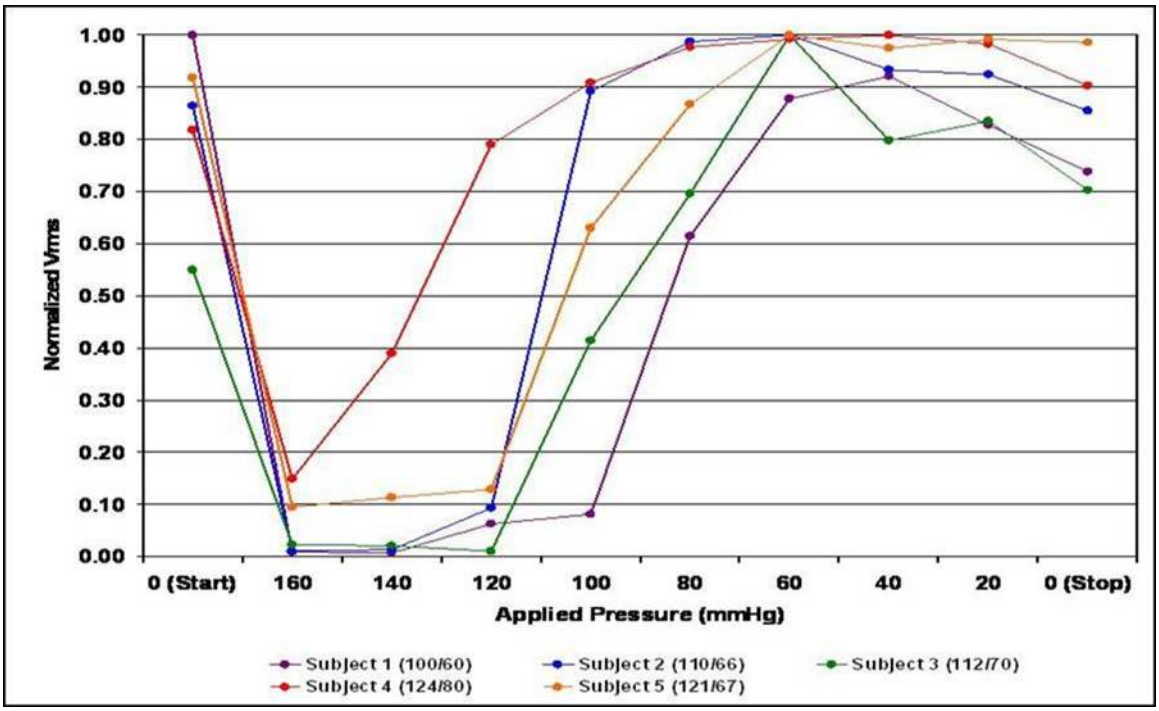

Figure 4.7: Normalized RMS Voltage vs. Applied Pressure– Arterial Processed Data

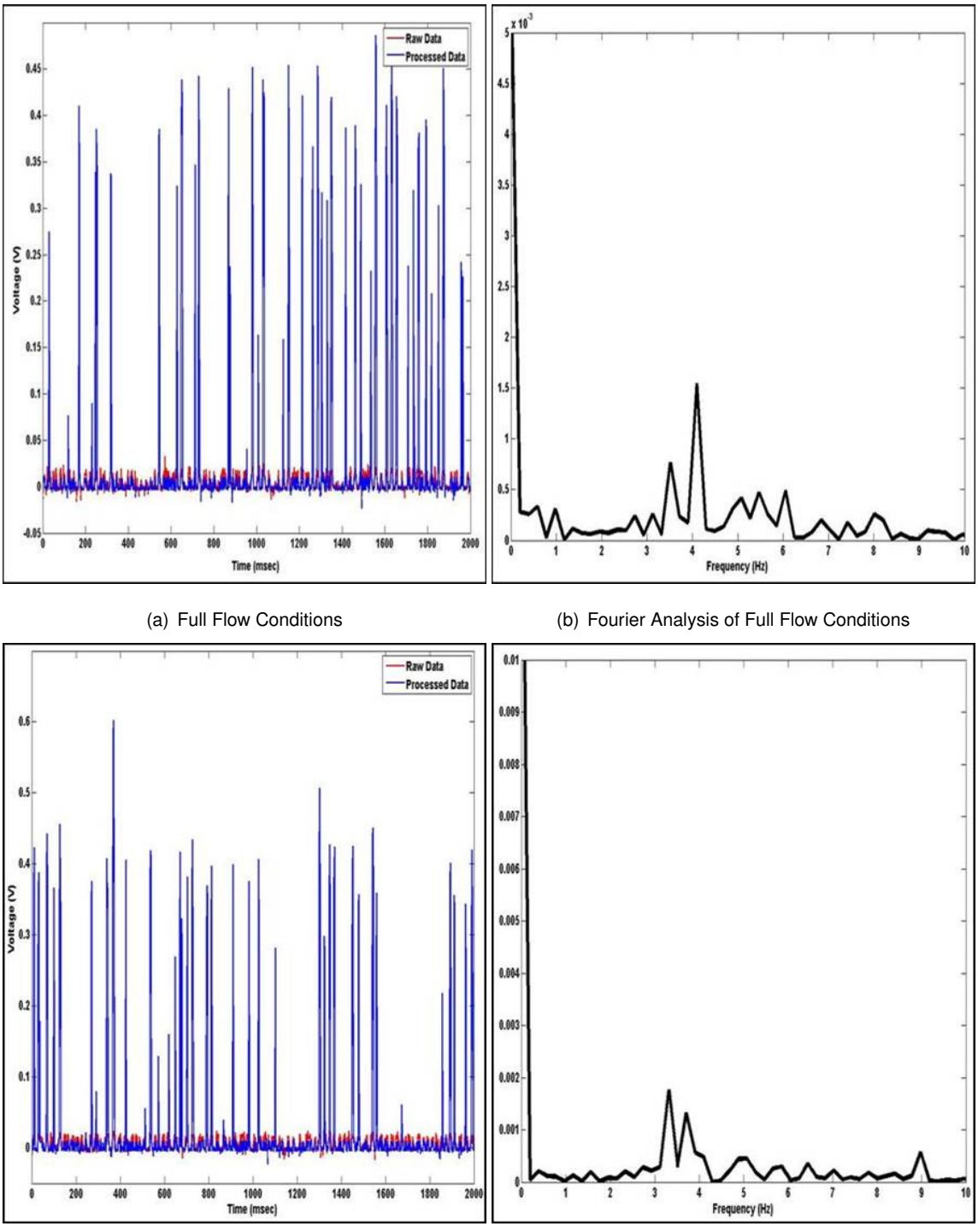

(a) Full Flow Conditions

(b) Fourier Analysis of Full Flow Conditions

(c) Zero Flow Conditions

(d) Fourier Analysis of Zero Flow Conditions

Figure 4.8: Influence of Applied Pressure on the Venous Pressure Waveform– Raw Data

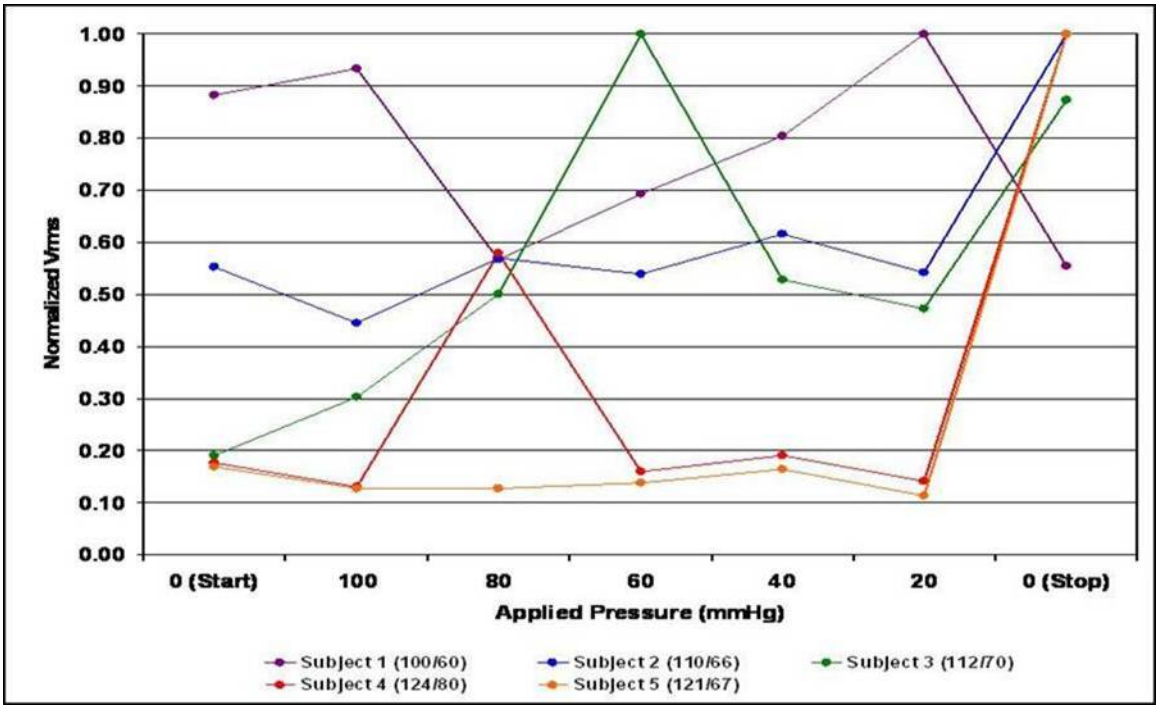

Figure 4.9: Normalized RMS Voltage vs. Applied Pressure– Venous Raw Data

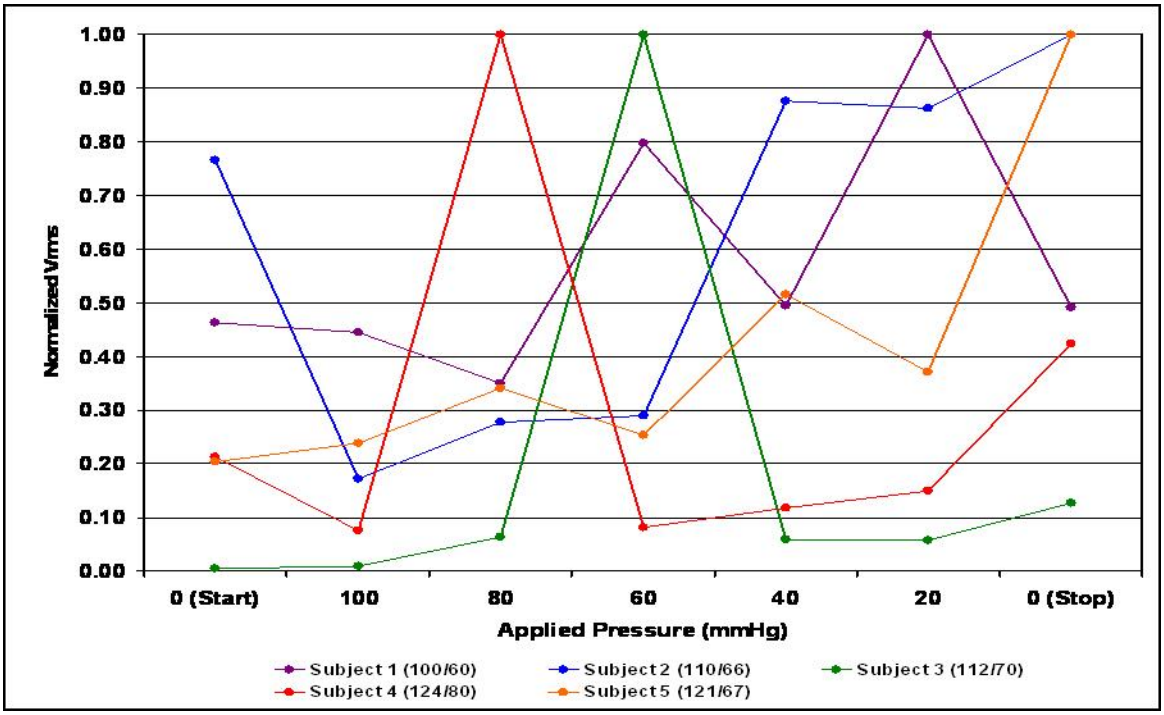

Figure 4.10: Normalized RMS Voltage vs. Applied Pressure– Venous Processed Data

of a pulse, although this level is generally below full flow conditions. Signal strength continues to increase until diastolic pressure is reached, and then appears to level off or drop slightly. Again, this is to be expected because full flow should be regained when the applied pressure falls below the diastolic pressure. Please note that for Subject 5, a final amplification of 11x was accidentally applied (i.e. versus 4.9x); this is not expected to affect the validity of the results, as all results are normalized. Additionally, the data obtained for Subject 5 is comparable to that of all other subjects.

The Acoustic Blood Flow Monitoring System is not able to detect venous blood flow. Sample full flow (i.e. 0 mmHg applied pressure– starting measurement) and zero flow (i.e. 100 mmHg applied pressure) pressure waveforms for Subject 5 are shown in Figure 4.8. When examining these traces, one can see that the full flow and zero flow conditions appear markedly similar (i.e. both appear to be noise). Additionally, the expected periodic changes due to breathing were not observed in the full flow signal. Fourier analysis of the full flow data shows that the strongest frequency component is well above the expected 0.2-0.3 Hz. This confirms that venous blood flow is not being measured.

Signal power also increases/decreases in a seemingly random fashion (see Figure 4.9 and Figure 4.10). This further supports the claim that venous flow is not being measured, as there should be a clear difference in signal strength between full, partial, and zero flow conditions. In fact, the signal actually grows stronger as pressure is increased from 0 mmHg to known zero flow conditions (i.e. $>$50 mmHg) in the majority of subjects tested. A large difference in starting and stopping RMS voltages (raw data) was also noted for Subjects 3, 4, and 5. This is not to be expected, as both measurements were taken with 0 mmHg of applied pressure. Such a large discrepancy was not noted when measuring changes in arterial flow. Additionally, the venous signal power and ambient noise signal power were of comparable magnitudes, indicating that the signal lay near the noise floor of the circuit.

4.2.2 Experiment 2– Effects of Array Displacement

Purpose

The purpose of this experiment is to verify the robustness of the Acoustic Blood Flow Monitoring System in the event that the microphone array is shifted from its home location (see Figure 4.11). This situation is likely to occur if the array is not initially positioned properly (i.e. slightly to one side of the main axis of the vessel), or if the array becomes displaced as a result of patient movement (i.e. shifting weight, walking, etc.).

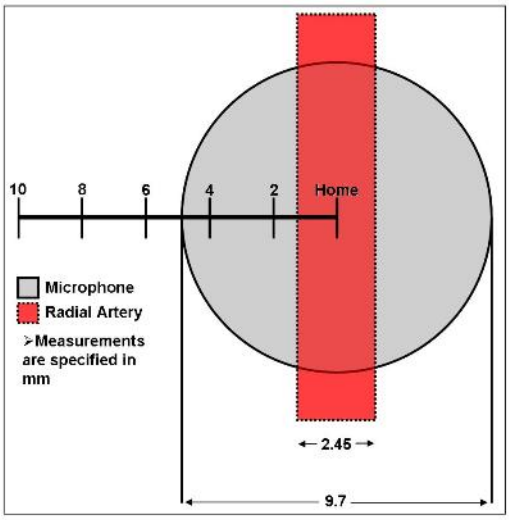

Figure 4.11: Setup for Array Displacement Experiment

Outline

The primary objective of this experiment is to quantify the effects of microphone array displacement. This will be accomplished by calculating the RMS voltage (i.e. indicator of signal power) and pulse rate at five different off-axis displacement distances. The experimental pulse rate will be compared to the subject's known pulse rate, and this data used to quantify the accuracy of the system. As displacement distance increases, the skin and subcutaneous tissue are expected to compound signal attenuation, resulting in a decrease in both signal power and accuracy.

The results of this experiment will also be used to determine if the microphone array could be attached over the compression stocking (i.e. versus underneath the stocking). During the first series of tests, no external pressure will be applied to the microphone array. Attaching the array over the stocking would be ideal because it would ease application and removal. If the pulse cannot be accurately recorded under this zero external pressure condition, the array will need to be placed under the stocking to improve contact. Placing the system underneath the stocking is undesirable because one would need to account for the differences in contact pressure resulting from the variable application of external pressure [19]. In the second series of tests, 20 mmHg of external pressure will be applied to the microphone; this will be used to simulate the pressure applied by a low-level medical grade compression stocking.

Methods

The subject's blood pressure and heart rate were measured using an automatic blood pressure monitor (OMRON IntelliSense Digital Wrist Blood Pressure Monitor, Model: HEM-609ECK). The cuff was then removed and the subject was asked to rest their right arm on a table with their palm facing up. The radial artery was palpated, and a mark was made to denote its location (i.e. home position). Five marks, spaced 2 mm apart, were drawn along a horizontal line extending medially from the radial artery (total length: 1 cm; see Figure 4.11). A modified blood pressure cuff (see Figure 4.12) was aligned so that the center of the microphone corresponded with the mark denoting the location of the radial artery. Please note that the microphone was held against the subject's bare arm in both test scenarios (i.e. not over a sleeve/stocking).

Figure 4.12: Modified Blood Pressure Cuff

For the first trial, the blood pressure cuff remained completely deflated (i.e. zero pressure condition). The subject's pulse was recorded for approximately 20 sec using the Acoustic Blood Flow Monitoring System (100 Hz sampling rate; final gain: 1x, 4.9x, 11x). MATLAB was used for data processing, storage, and display purposes. Upon completion of the first trial, the blood pressure cuff was inflated to 20 mmHg, and a second recording was made in the same manner as previously described. The microphone was moved in 2 mm increments, and the entire process repeated. The microphone was then removed from the subject's wrist, and an ambient noise recording was made. Each measurement was saved in a separate file.

Data Analysis

The RMS voltage of the signal was calculated at each displacement distance for both pressure levels. These values were normalized against the RMS voltage of the ambient noise. The normalized RMS voltage data was then pooled for each displacement measurement, and an overall average computed. This averaged data was plotted against displacement location (note: data was further normalized against the largest measured RMS voltage for graphical display purposes).

The average pulse rate over 10 beats was calculated. The percent error between the calculated and actual pulse rate (as measured by the automatic blood pressure cuff) was determined. This was used to indicate the quality of the collected data. A t-test was used to determine if there was a significant difference in signal power and accuracy between the 0 mmHg and 20 mmHg external pressure conditions (i.e. data for which a pulse was not detected at either pressure level was excluded from this analysis).

Results

The results of this experiment highlight the difficulty in determining the home location (i.e. location of the strongest pulse), and the importance of proper initial alignment. Sample home (0 mm displacement, 20 mmHg applied pressure) and displaced arterial pressure waveforms (8 mm displacement, 20 mmHg applied pressure) for Subject 2 are shown in Figure 4.13. As expected, the signal was lost when the microphone was significantly shifted from the home location. At the 8 mm displacement mark, no portion of the microphone would be expected to overlap the artery.

Given the high level of disagreement between the experimental and measured pulse rates, proper alignment may not have been achieved for Subjects 4 and 5. For both of these subjects, a pulse signal could not be obtained beyond the 0 mm mark. This may indicate that the true home location was located distal to the experimental home location. Of note is the fact that these subjects had a higher density of arm hair in the region where the pulse was being measured. As the subjects' arms were not shaved, this hair may have prevented good contact between the microphone and skin.

Initial misalignment may also have been and issue for Subject 3. A significant increase in signal power was noted at the 2 mm mark when 20 mmHg of external pressure was applied; the signal power essentially remained constant between the 0 mm and 2 mm mark when no external pressure was applied. Subject 3 was the only subject to exhibit this pattern, and it does not make physical sense for the pulse to be stronger as one moves off the artery. In light of this, it is reasonable to suppose that the true home position was the 2 mm mark, with the 0 mm mark actually being located

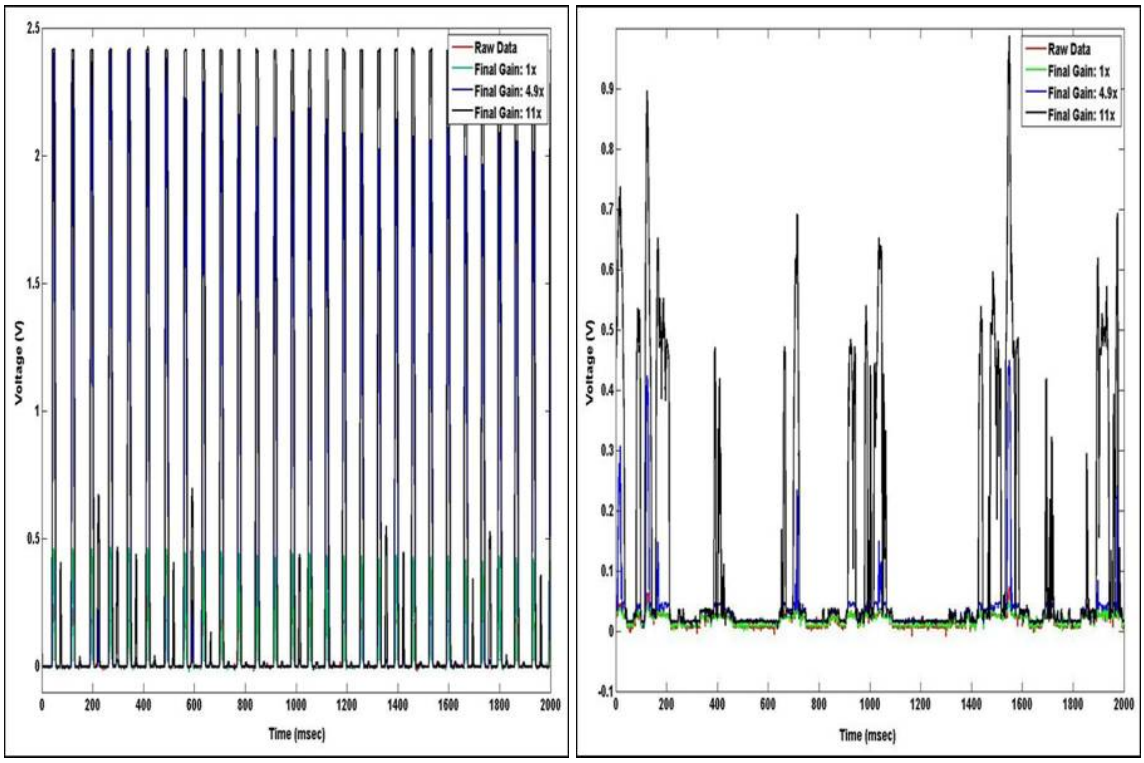

(a) Home Position (clear pulse waveform) (b) 8 mm Displacement (noise from breathing)

Figure 4.13: Affect of Microphone Positioning on Recorded Signal

distal to this site. Subsequent analysis has been carried out using this assumption (i.e. all data was shifted -2 mm; no signal was assume to exist at 10 mm, as supported by the original data).

For all subjects tested, no pulse signal was obtained after 4 mm of displacement (see Table 4.2). Signal decay was found to approximate an exponential curve (see Figure 4.14 and Figure 4.15). When no external pressure was applied, the signal was lost beyond the 2 mm mark in four out of five subjects. Of note is the fact that Subject 1 (i.e. the only subject for whom a signal was obtained at the 4 mm mark) had no arm hair in the region where the pulse was being measured; this was not true of any other subject. When 20 mmHg of external pressure was applied, the signal was lost between the 2 mm mark in three out of five subjects. This may provide evidence for supplying external pressure, as the range of the microphone was extended by 2 mm in one subject (i.e. subject 3). When a pulse was detected, signal power was greater when external pressure versus no external pressure was applied ($p = 0.05$); this presumably means that the pulse would be easier to detect. No difference was noted in terms of accuracy.

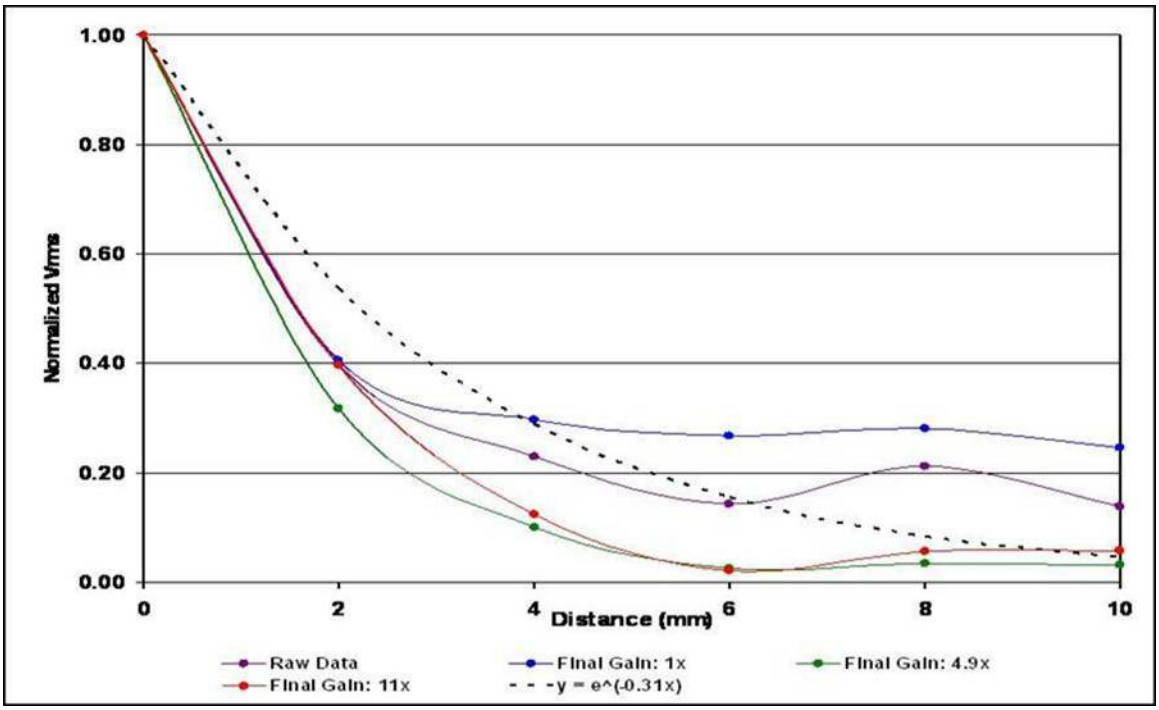

Figure 4.14: Average Normalized RMS Voltage vs. Distance– 0 mmHg Applied Pressure

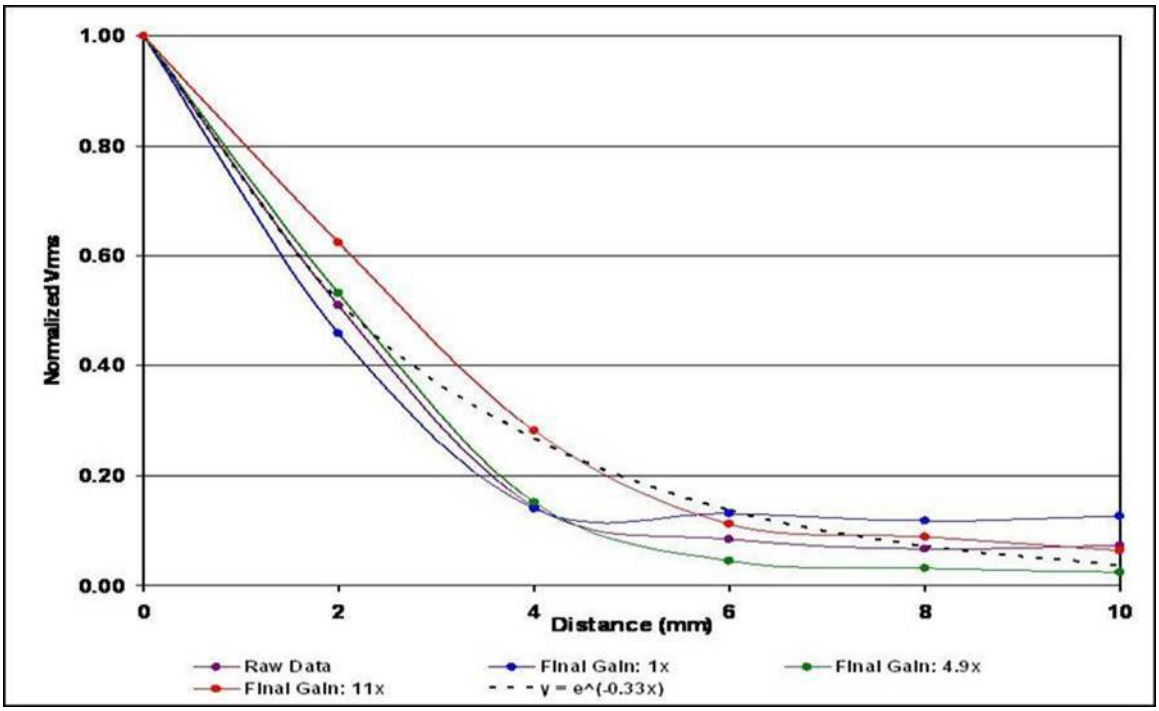

Figure 4.15: Average Normalized RMS Voltage vs. Distance– 20 mmHg Applied Pressure

Table 4.2: Microphone Range Data

Subject		Displacement Distance					
		0 mm	**2 mm**	**4 mm**	**6 mm**	**8 mm**	**10 mm**
1	0 mmHg	P	P	P	N	N	N
	20 mmHg	P	P	P	N	N	N
2	0 mmHg	P	P	N	N	N	N
	20 mmHg	P	P	N	N	N	N
3	0 mmHg	P	P	N	N	N	N
	20 mmHg	P	P	P	N	N	N
4	0 mmHg	P	N	N	N	N	N
	20 mmHg	P	N	N	N	N	N
5	0 mmHg	P	N	N	N	N	N
	20 mmHg	P	N	N	N	N	N

** P = pulse detected, N = no pulse detected*

4.3 Discussion

The Acoustic Blood Flow Monitoring System can acceptably resolve arterial blood flow. There is a clear difference in signal power between known full and zero flow conditions, with increases/decreases in strength following predictable patterns. Fourier analysis of the raw data reveals a strong power band in the expected frequency range (i.e. 1-1.5 Hz). This system is not, however, capable of detecting venous blood flow. Signal strength increases/decreases in a seemingly random fashion, with no clear difference between known full and zero flow conditions. Additionally, signal power does not reside in the frequency range of interest (i.e. 0.2-0.3 Hz).

The Acoustic Blood Flow Monitoring System also fails in terms of robustness, and cannot perform acceptably in the event of array displacement. When the microphone array is shifted off-axis in excess of 4 mm, the pressure waveform can no longer be accurately sensed. In three out of five subjects, the pulse signal was lost after only 2 mm of displacement. Additionally, gross inaccuracies were noted when exact alignment was not attained. Achieving proper alignment was extremely difficult, with setup times often exceeding 5 min. This situation would be exacerbated at the femoral artery and vein, as the pressure waveform is expected to be significantly smaller at these locations.

Experimental evidence also points to the need to place the array under the stocking in order to improve microphone contact. Although there is not a significant difference in system accuracy with the application of external pressure, the magnitude of the recorded pulse waveform is significantly greater. This serves to raise the signal further above the noise floor of the circuit, and may help to extend the range of the microphone. Evidence to support this claim can be found upon careful examination of the data for Subject 3, as no pulse was recorded with 0 mmHg of pressure and a

pulse was recorded with 20 mmHg of pressure at the 4 mm displacement mark. System accuracy could also be improved by shaving the area over the vessel of interest.

In conclusion, the Acoustic Blood Flow Monitoring System cannot be used to measure arterial and venous blood velocity for this application. The system is not sensitive enough to accurately resolve venous flow, and is not robust in the face of array displacement. Other options, such as Doppler ultrasound, should be explored.

Chapter 5

Application of Bio-Impedance Analysis to Edema Monitoring

Edema reduction has previously been classified as a necessary component for ulcer healing (see Section 3.2.2). The state of edema can be quantified using bio-impedance analysis to monitor changes in leg volume. Impedance analysis techniques take advantage of the fact that the resistance of an object is known to vary inversely with cross-sectional area. Assuming that the length of the object remains constant, differences in volume (i.e. resistance) can be measured by applying a known current and monitoring the respective change in voltage [33].

With respect to bio-impedance, two pairs of electrodes are attached to the body as shown in Figure 5.1(i.e. tetra-polar configuration). This electrode configuration serves to eliminate parasitic impedances (i.e. from the skin) and decreases system sensitivity to electrical events close to the electrodes [33, 25]. A high-frequency (i.e. 10-100 kHz), low amplitude AC current is passed between the outer pair of electrodes, and changes to this signal are measured by the inner pair of electrodes (see Figure 5.1). A stimulating frequency of 50 kHz is traditionally used, although different properties can be measured by varying this frequency [33].

In practice, impedance plethysmography can easily be implemented using low-cost equipment that requires minimal calibration. Continuous, on-line monitoring is also possible, making it ideal for clinical use. As a result, bio-impedance analysis is now widely used to access the health of the circulatory system, and has been used to detect deep venous thrombosis, chronic venous insufficiency, and peripheral arterial insufficiency [33, 25].

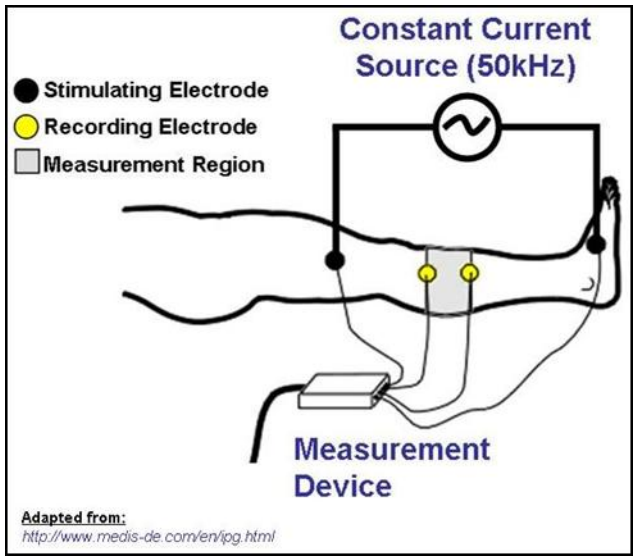

Figure 5.1: Tetra-polar Electrode Configuration for the Lower Leg

5.1 Circuit Design

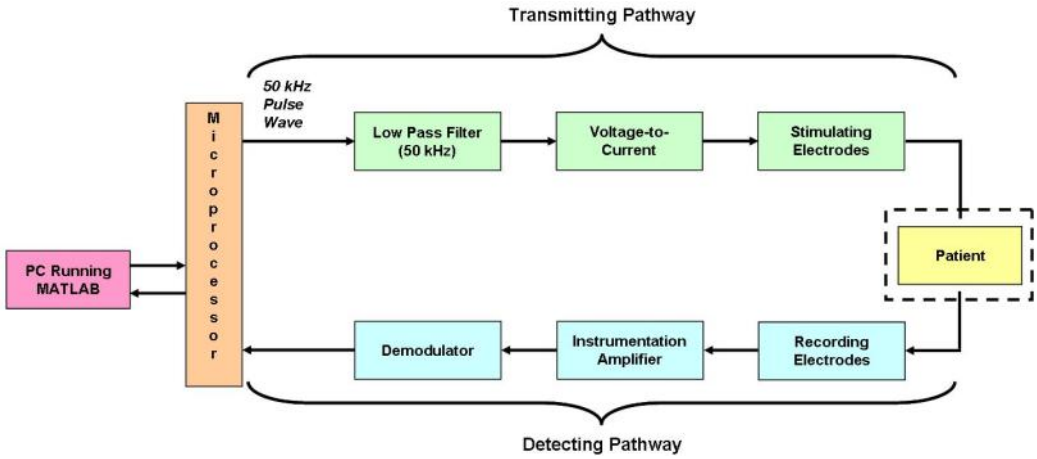

Figure 5.2: Edema Monitoring System

The Edema Monitoring System circuitry can be broken down into two modules- (1) transmitting and (2) detecting. The transmitting module consists of the circuitry required to pass a small, high-frequency AC signal through the limb. The detecting module is comprised of those elements needed to sense a change in the amplitude of the received signal. The volume of the limb can be determined using Ohm's Law. Please refer to Figure 5.2 for a layout of the Edema Monitoring System, and Appendix B for the complete circuit schematic.

Many of the errors associated with current tetra-polar systems can be traced to common-mode effects and stray capacitance [34]. An effort was made to reduce effects from these and other sources of error by selecting components with the following characteristics [34, 35]:

- *Current Source*: high output impedance
- *Electrodes*: abraid the skin and use conductive gels/pastes to improve contact; ensure electrode separation is at least equivalent to one limb diameter (i.e. to avoid approaching the two electrode model)
- *Sensor*: high input impedance; large bandwidth; high Common Mode Rejection Ratio (CMRR)
- *Data Processing*: A/D resolution of 12-bits or higher

Again, power consumption, size, and cost were also considered when selecting components for the Edema Monitoring System.

5.1.1 Transmitting Circuit

In order to generate a 50 kHz AC signal (i.e. sine wave), a microprocessor (MSP430F149, Texas Instruments) is used to produce a 50 kHz square wave. This square wave is then low-pass filtered (4^{th} order Butterworth filter, cutoff: 50 kHz) to produce a sine wave, which serves as an input to a precision current source. The current source is implemented using the enhanced Howland topology (see Figure 5.3). This design was selected over other current source options (i.e. current mirror type or multi-op-amp feedback type current source) because it is characterized by a high output impedance and requires relatively few components [36, 37, 38].

In the enhanced Howland circuit, the current output is a function of the voltage input, and the output impedance is a function of the selected resistor values [36, 37, 38]. Using the typology specified in Figure 5.3, the following equations are obtained [36]:

$$I_{out} = \left(\frac{R_2+R_3}{R_1R_3'}\right)V_{in} + \left(\frac{(R_1'R_2-R_1R_2')-\left(R_1'R_3-R_1R_3'\right)}{R_1R_3'\left(R_1'+R_2'\right)}\right)V_{out}$$

$$R_{out} = \frac{R_1R_3'(R_1'+R_2')}{R_1'(R_2+R_3)-R_1\left(R_2'+R_3'\right)}$$

If one sets $R_1 = R_1' = R_i$, $R_2 = R_2' = R_f$, and $R_3 = R_3' = R_s$, these equations simplify to:

$$I_{out} = V_{in}\left(\frac{R_f+Rs}{R_iR_s}\right)$$

$$R_{out} = \frac{R_iR_s\left(R_i+R_f\right)}{R_i\left(R_f+R_s\right)-R_i\left(R_f+R_s\right)} = \infty$$

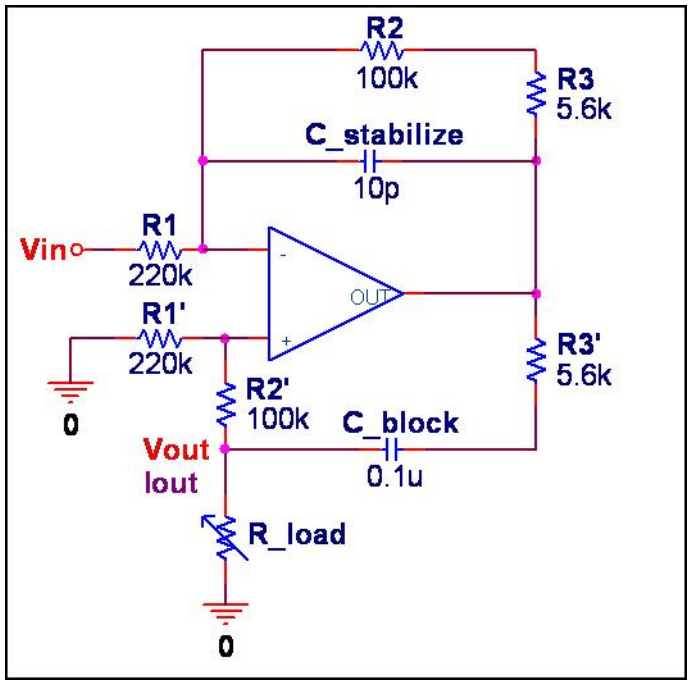

Figure 5.3: Enhanced Howland Current Circuit

In other words, the output impedance of the circuit approaches infinity if all resistor pairs are perfectly matched. Small values of R_s help to improve load range, and at least one source recommended that $R_s << R_i, R_f$ [36, 39]. Additionally, large values of R_i and R_f serve to keep the quiescent current low, allowing for better power efficiency. The resistor values as specified in Figure 5.3 were selected based upon these recommendations. The selected resistor values also limit current to less than 1 mA RMS under normal operating conditions (i.e. industry standard) and ensure that the supplied current will not exceed the safety limitations imposed by IEC 2007 60601-1 guidelines (see Appendix B). The 10 pF capacitor in the negative feedback loop was added to aid in circuit stability [36, 38]. The final circuit also includes 0.1 μF DC-blocking capacitor for patient safety (i.e. a DC voltage being applied to the skin may result in irritation or burning) [34].

5.1.2 Detecting Circuit

In order to raise the small incoming signal above the noise floor of the circuit, the output of the sensing electrodes is routed through an instrumentation amplifier (INA332, Texas Instruments). This amplifier is characterized by a high input impedance, large bandwidth, and good CMRR. The output of the instrumentation amplifier reflects the voltage across the measurement area. If the

supplied current is known and assumed to remain constant, the impedance of the segment can be calculated using Ohm's Law:

$$V_{segment} = I_{body} * R_{segment}$$

where $V_{segment}$ is the voltage sensed using the instrumentation amplifier, I_{body} is the current supplied by the enhanced Howland circuit (see Section 5.1.1), and $R_{segment}$ is the impedance of the lower leg (i.e. impedance and volume are inversely related). Therefore, changes in impedance are indicated by an increase/decrease in the measured signal amplitude (i.e. DC level). In order to recover the DC portion of the signal, demodulation techniques can be used. A simple demodulator can be formed by placing a low-pass filter (i.e. with a low cutoff frequency) in series with a full-wave rectifying circuit. In order to achieve operation at 50 kHz, high speed, small signal diodes (BAW62, Philips Semiconductors) and large bandwidth op-amps with a fast slew rate (FAN4274, Fairchild Semiconductor) were selected. The demodulated signal is then sampled at a rate of 100 Hz by the microprocessor (MSP430F149, Texas Instruments; 12-bit A/D), which communicates serially with a PC. Further processing and analysis are carried out using MATLAB.

5.2 Experiments

Two experiments were conducted in order to test the accuracy of the system under laboratory conditions (Section 5.2.1) and in actual use (Section 5.2.2). In the first experiment, a decade box was used to simulate the response of the lower leg to an applied AC signal. The decade box allowed for the fine adjustment of known resistances over the expected range of impedances. In the second experiment, electrodes were applied to the subject's lower leg in the configuration commonly selected for vascular assessment. This situation is identical to real-world use.

5.2.1 Experiment 1– Measuring Small Changes in Resistance

Purpose

The purpose of this experiment is to verify that the Edema Monitoring System can accurately measure small changes in resistance. The average resistance of the human body is known to be 450 Ω [40]. Literature concerning the average resistance of the lower leg, however, varies significantly. Resistances as low as 20-80 Ω [41, 42] to values on the order of 150 Ω [4, 43] have been reported.

Outline

The output of the Edema Monitoring System will be measured when a known load is applied. The resistance of the load will be adjusted from 0-200 Ω in 5 Ω increments in order to accomodate the range of resistances that have been cited for the lower leg [4, 41, 42, 43]. The average voltage level for a particular resistance will be computed, and a calibration curve generated. The sensitivity of the system (i.e. the slope of the calibration curve) will then be calculated. This information will be used to determine if the Edema Monitoring System can acceptably detect small changes in resistance.

Methods

The positive stimulating and recording leads of the Edema Monitoring System were attached to the positive terminal of a decade box. The negative stimulating and recording leads of the Edema Monitoring System were attached to the ground terminal of a decade box. The resistance of the load was set to 0 Ω. The resulting signal was recorded for approximately 5 sec (100 Hz sampling rate). The resistance was then adjusted in 5 Ω increments until a resistance of 200 Ω was achieved. A measurement was made at each resistance level using the same process as previously described (i.e. total of 41 measurements). This procedure was then repeated 4 more times (i.e. total of 5 trials), with a minimum of 30 min between trials. For each trial, the system was re-started in order to account for heating effects.

Data Analysis

The average voltage level for each resistance value was calculated for all trials. This data was examined in order determine if all measurements were repeatable over the expected range of lower leg impedances (i.e. 20-200 Ω). All results were then consolidated into one data set, and this set used to generate a calibration curve for the system. The slope of the calibration curve was computed and used to determine the sensitivity of the system.

Results- System Designed Assuming Impedance of 20-200 Ω (Configuration A)

The Edema Monitoring System can accurately detect small changes in resistance. All measurements were repeatable over the range of expected resistances (see Figure 5.4). The response of the system was linear from 20-200 Ω (R^2=1; see Figure 5.5). At very small resistance

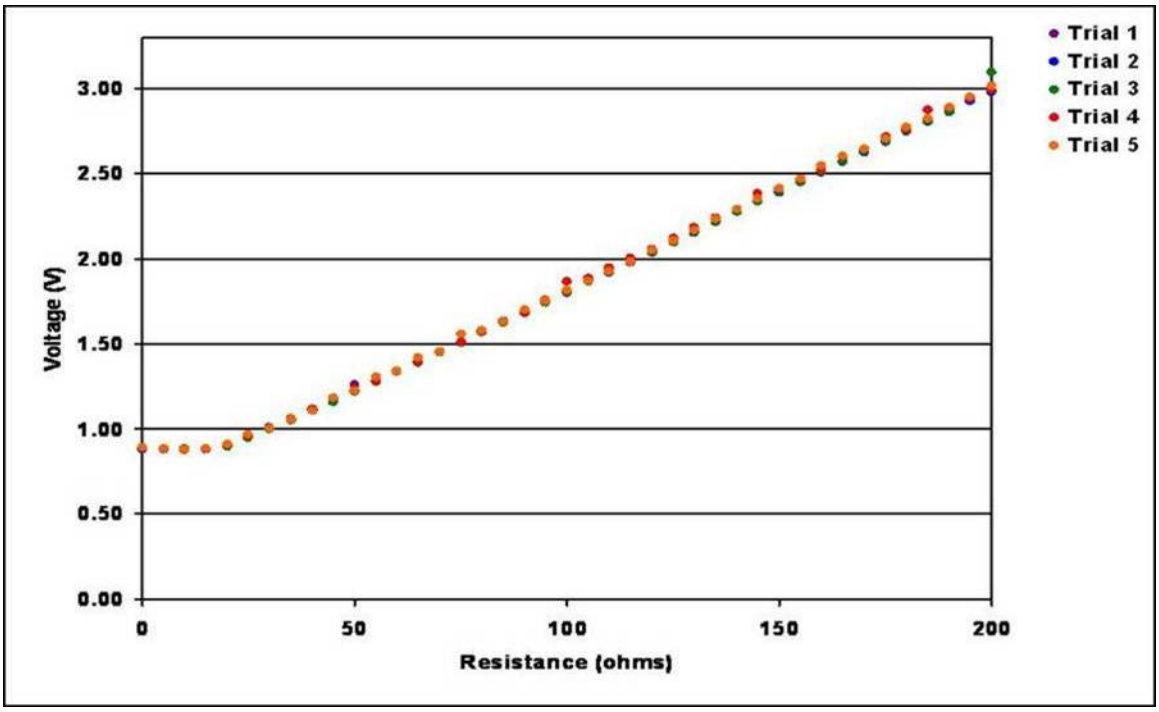

Figure 5.4: Voltage vs. Resistance (Configuration A): Trials 1-5

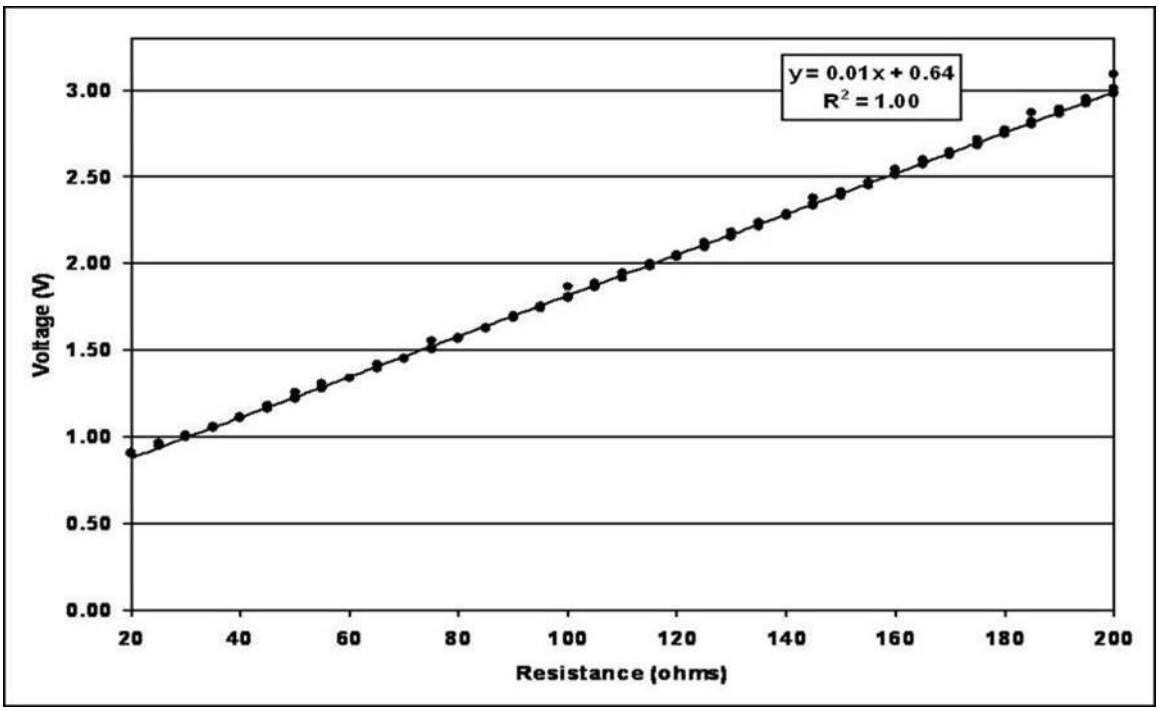

Figure 5.5: Calibration Curve (Configuration A)

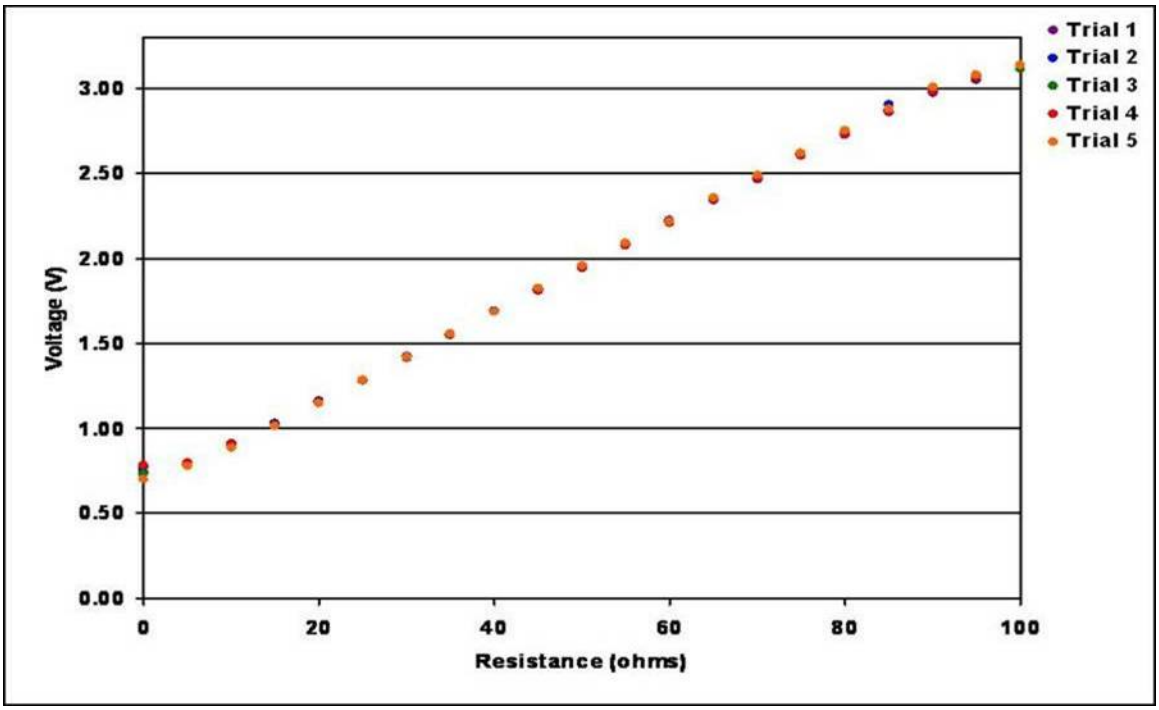

Figure 5.6: Voltage vs. Resistance (Configuration B): Trials 1-5

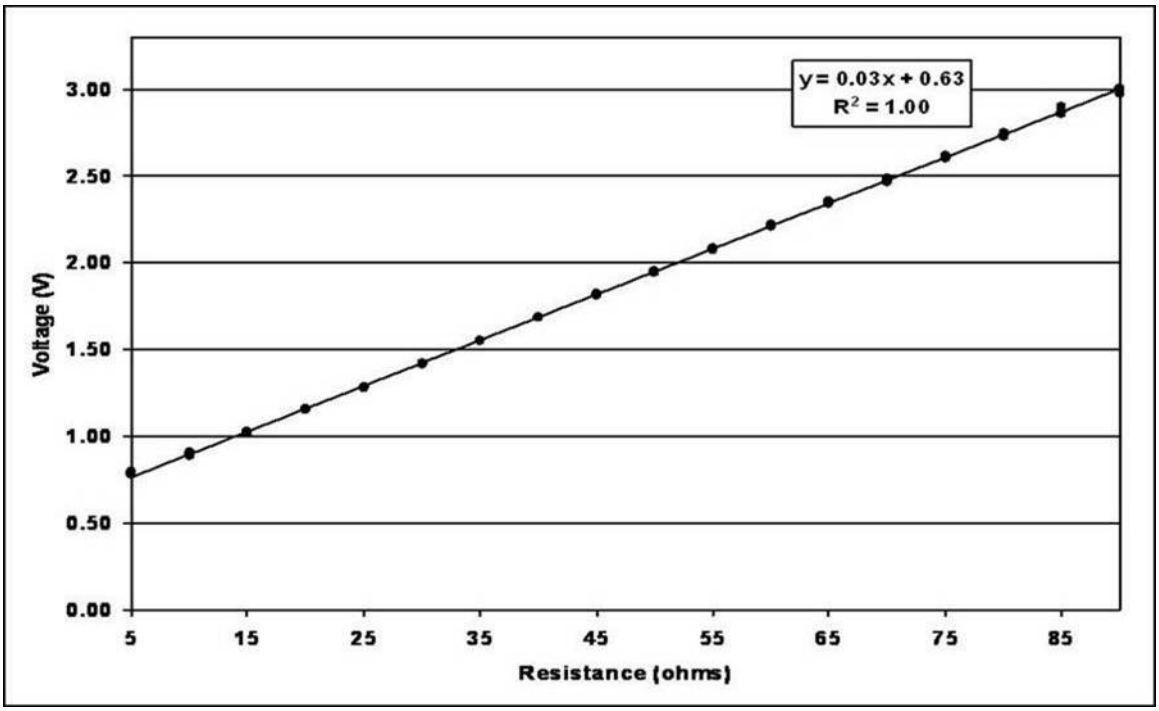

Figure 5.7: Calibration Curve (Configuration B)

values (i.e. 0-20 Ω), however, the system exhibited non-linear behavior. Based upon these results, the following calibration curve was obtained (please note that this curve was computed for resistance values extending from 20-200 Ω):

$$V = 0.01 * R + 0.64\Omega$$

where V is the measured voltage (in volts) and R is the resistance (in ohms). This indicates that the system has a sensitivity of 0.01 V/Ω. Variability in the measured resistances ranged from 0.00-0.05V, with a rough trend towards increasing variability with increasing resistance beginning at approximately 85 Ω (a variance of 0.05V was recorded at a resistance of 200 Ω).

Results- System Designed Assuming Impedance of 20-80 Ω (Configuration B)

When the impedance of the lower leg was actually measured using the Edema Monitoring System (see Section 5.2.2), resistance values of 28-32 Ω were observed. This indicates that the range of 20-80 Ω cited by Seo et al. in [41, 42] seems most appropriate. In order to account for this difference, the Edema Monitoring System was altered to provide a higher resolution in this range (i.e. an amplification of 170x versus 72x was applied).

As with the previous configuration, all measurements were repeatable over the range of resistances tested (see Figure 5.6). The response of the system proved to be highly linear from 5-90 Ω (see Figure 5.7). A new calibration curve described by the following equation was obtained (please note that this curve was computed for resistance values extending from 5-90 Ω):

$$V = 0.03 * R + 0.63\Omega$$

The sensitivity of the new configuration was calculated to be 0.03 V/Ω, a 0.02 V/Ω improvement over the previous configuration. Variability was also reduced to 0.00-0.02V. Again, there was a trend towards increasing variability with increasing resistance beginning at approximately 40 Ω (i.e. a variance of 0.02 V was recorded at a resistance of 85 Ω).

5.2.2 Experiment 2– Measuring Small Changes in Leg Volume

Purpose

The purpose of this experiment is to confirm that the Edema Monitoring System can acceptably resolve small changes in leg volume.

Outline

The impedance of the lower leg will initially be measured under resting conditions to establish a baseline. A blood pressure cuff will then be placed around the upper leg and inflated to 100 mmHg; an impedance measurement will be taken under these conditions. This pressure is sufficiently low to allow for arterial blood flow to continue (i.e. blood can reach the lower leg), but high enough to block venous return (i.e. blood cannot travel back to the heart). As a result, blood begins to pool in the lower leg, thus mimicking the conditions associated with the initial onset of superficial venous hypertension. The impedance of the leg is expected to be lower in the pressurized state due to an increase in leg volume. The pressure on the upper leg will then be released, and a final impedance measurement taken in order to track recovery.

Methods

The impedance of the lower leg was measured using the Edema Monitoring System. Four electrodes (CLEARTRACE ECG Electrodes, ConMed) were applied to the lateral side of the subject's leg using a standard configuration (see Figure 5.8). A constant current of 95 μA RMS was applied through the outer pair of electrodes (i.e. located on the mid-thigh and foot) [44]. The voltage potential was recorded between the inner pair of electrodes (i.e. located on either side of the calf). Care was taken to maintain similar electrode placement over the course of the testing period.

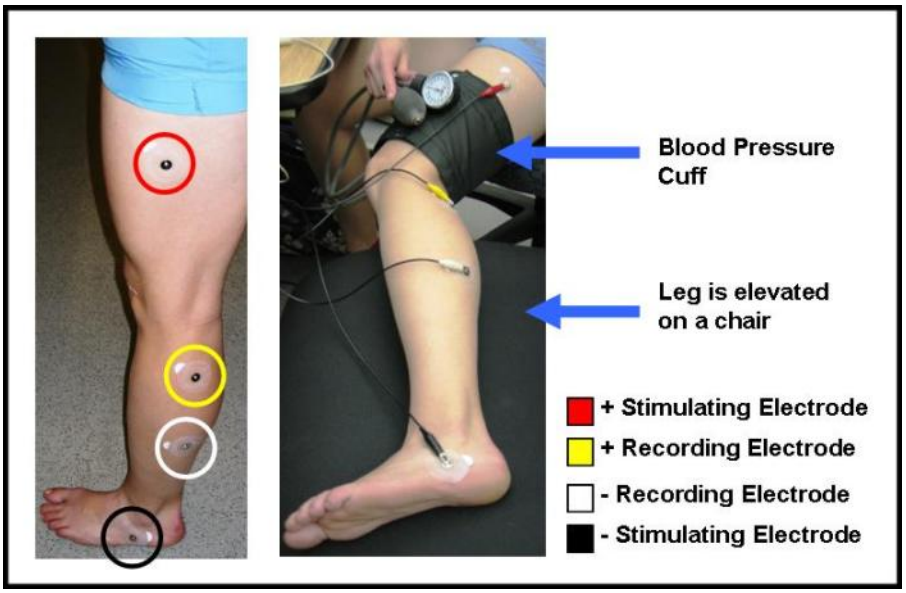

Figure 5.8: Electrode Positions and Experimental Setup

A manual blood pressure cuff was placed around the subject's lower thigh, and the leg elevated to hip-height (see Figure 5.8). The impedance of the lower leg was measured for 1 min (i.e. resting measurement). The cuff was then inflated to 100 mmHg, and the impedance of the lower leg measured for 1 min (i.e. swelling measurement). The pressure was then released, and the impedance of the lower leg measured for 1 min (i.e. recovery measurement). Please note that the impedance of the lower leg was also measured during inflation and deflation of the cuff, but these measurements were not used for analysis purposes. This process was repeated 4 more times (i.e. total of 5 trials), with a minimum of 30 min between each trial to ensure full recovery.

Data Analysis

A plot of impedance versus time was created by splicing together each measurement segment (i.e. resting, cuff inflation, swelling, cuff deflation, and recovery). The data was then passed through a low-pass filter (second-order Butterworth filter, cutoff = 0.1 Hz) to facilitate observation of overall trends. The resting, swollen, and recovered measurement blocks were then divided into 5 sec intervals, and the average of each interval computed (note: this is the measurement protocol that will be implemented in the actual system). A second plot of impedance versus time was then created using this data.

The average resting, swollen, and recovered voltage potentials were also computed for each trial. The voltage potential is related to leg volume by:

$$V = I * \frac{1}{Volume}$$

where V is the average voltage potential (in volts) and I is the constant current being applied between the two outer electrodes. These values were compared using a series of t-tests.

Results

The Edema Monitoring System was able to reliably track small changes in leg volume resulting from artificially-induced swelling. An example of the Edema Monitoring System output recorded during this experiment is shown in Figure 5.9. The 5 sec interval data (i.e. adopting the measurement protocol which will be used in the actual system) is shown in Figure 5.10. Clear differences in the measured voltage potentials for each condition are evident in these plots.

The average voltage level recorded between the inner electrodes during resting, swollen, and recovered conditions is shown in Table 5.1. In all cases, the recorded voltage was largest during

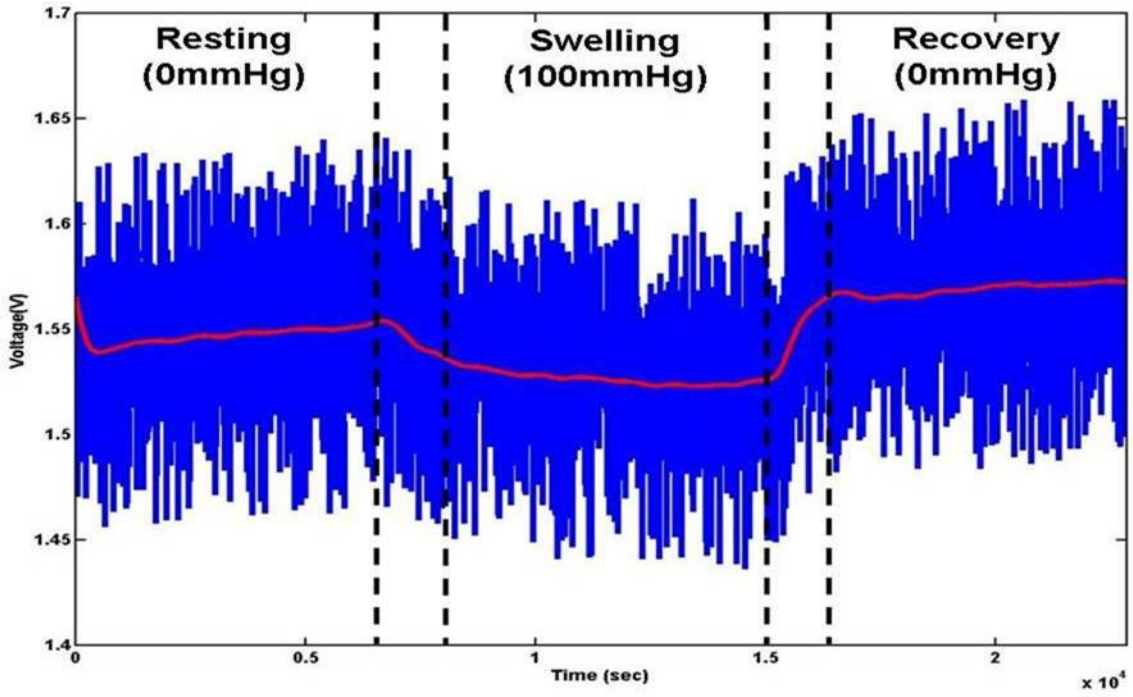

Figure 5.9: System Response to Artificially-Induced Swelling

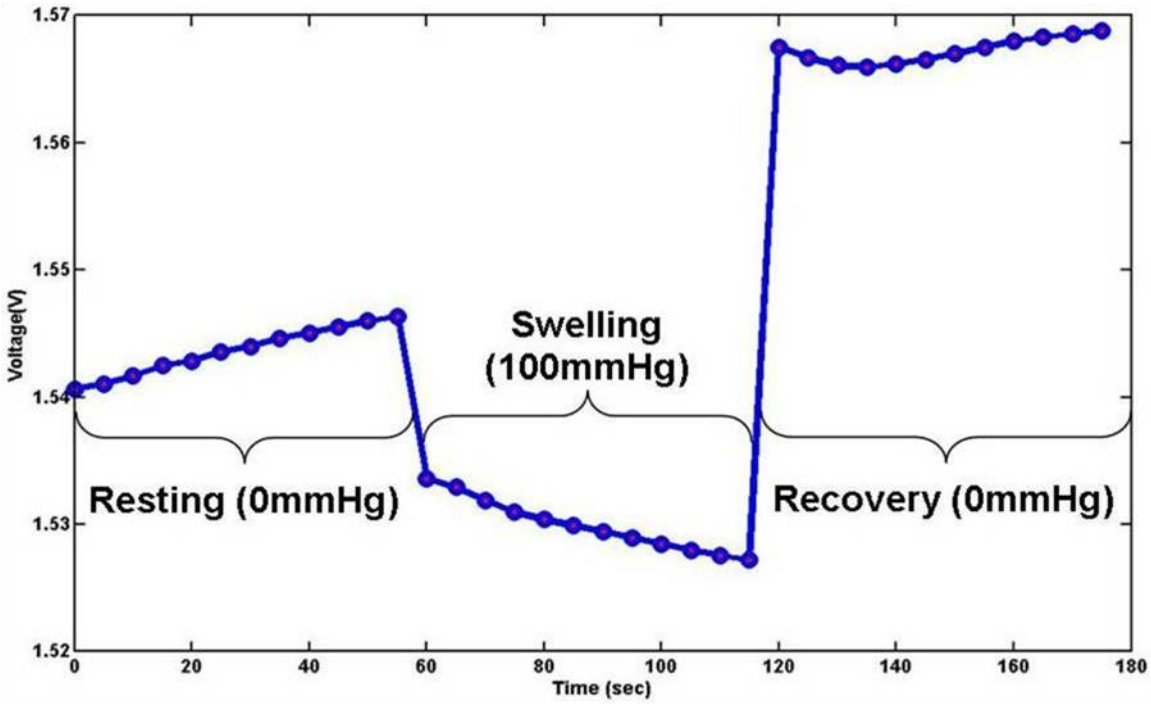

Figure 5.10: System Response Assuming 5 sec Measurement Protocol

Table 5.1: Average Voltage Levels for Each Volume State

Trial	Resting (V)	Swelling (V)	Recovery (V)
1	1.55	1.53	1.57
2	1.56	1.55	1.58
3	1.48	1.49	1.53
4	1.53	1.51	1.56
5	1.52	1.50	1.54

the recovered condition. This difference was found to be significant with respect to both the resting (ρ=0.005) and swollen (ρ=0.00002) conditions. This spike upon pressure release was also noted in the first experiment conducted with the Acoustic Blood Flow Monitoring System (Section 4.2.1), which used a similar protocol. Furthermore, with the exception of Trial 3, the recorded voltage was larger during resting versus swelling conditions. The data for Trial 3 is suspect, as the average voltage levels are lower for all three conditions as compared to the other trials. This may indicate poor contact between the electrodes and the skin. Despite this anomaly, a significant difference between resting and swollen conditions was still found (ρ=0.03).

5.3 Discussion

The Edema Monitoring System can accurately measure small changes in impedance. Based upon the values cited for lower leg impedance, the original system was designed to measure resistances ranging between 20-200 Ω [4, 41, 42, 43]. The output of this system proved to be highly linear and predictable in this range, with a sensitivity of 0.01 V/Ω. Variability in the measured resistances, however, served to decrease system resolution. Variability was found to roughly increase beginning at 85Ω, and reached a maximum of 0.05 V at a resistance of 200 Ω.

When the actual impedance of the lower leg was measured using the Edema Monitoring System, values of 28-32 Ω were reported. Based upon these measurements, the decision was made to alter the Edema Monitoring System to reflect a more realistic impedance range of 20-80 Ω, as reported by Seo et al. [41, 42]. The newly configured system proved to be highly linear and predictable in the range of 5-90 Ω. Sensitivity was improved to 0.03 V/Ω, and variability reduced to a maximum of 0.02 V (i.e. an increasing trend in variability was noted beginning around 45 Ω).

The Edema Monitoring System is also able to accurately detect small changes in leg volume resulting from artificially-induced swelling. When venous return from the lower leg was blocked, there was a statistically significant difference in the recorded voltage potential. The recorded poten-

tial was lowest during swelling, indicating a decrease in resistance to current flow resulting from an increase in volume. Additionally, volume changes were apparent upon examination of the voltage trace.

In conclusion, the Edema Monitoring System was found to acceptably measure small changes in impedance under both laboratory and realistic conditions. The only cause for concern is related to the integrity of the contact between the skin and the electrode. As was observed in Trial 3 of the second experiment, poor contact might result in lower quality results (i.e. small changes may not be accurately resolved). In actual use, contact may be improved because the compression stocking would serve to hold the electrode against the skin.

Chapter 6

Conclusions and Future Work

The design of an intelligent compression stocking for the purposes of improving ulcer healing has been described in this thesis. A closed-loop control system has been proposed wherein physiological data is fed back to the system in order to allow for dynamic pressure regulation. After careful consideration, it was determined that two parameters– (1) blood flow velocity and (2) the state of edema– would need to be measured in order to quantify stocking performance.

Blood flow velocity serves as an indicator of nutrient delivery and waste removal to the ulcer site. Additionally, low venous flow velocity is associated with dangerous clot formation. The use of an acoustic array for the purposes of measuring arterial and venous blood flow velocity was explored in Chapter 4. This technique failed both in terms of accuracy and robustness. A suitable alternative for quantifying flow velocity is currently being tested (see Section 6.1.1).

Edema reduction is also closely tied to ulcer healing. The use of bio-impedance analysis for quantifying the state of edema was investigated in Chapter 5. This technique was found to acceptably resolve small changes in leg volume resulting from artificially induced swelling. Additionally, the system was found to be highly linear and predictable over the range of expected impedances.

6.1 Future Work

Prior to initial prototyping, an acceptable means by which to measure arterial and venous blood flow velocities must be found. From here, the project can take many directions. For example, additional sensing capabilities could be added, actuation improved, and the technology expanded to encompass all medical compression stockings. Each of these avenues is discussed in detail in the following sections.

6.1.1 Using Doppler Ultrasound to Measure Blood Flow Velocity

As previously described in Section 3.2.1, Doppler ultrasound can be used to measure both arterial and venous blood flow velocity. Engineers at the Center for Robotics and Intelligent Machines are currently investigating the use of continuous-wave (CW) Doppler for portable-wear applications. To review, CW systems utilize two matched piezo-electric crystals– one for transmitting a high frequency sound wave through the subcutaneous tissue and one for detecting the return wave. Changes in blood velocity are resolved by calculating the phase shift between the transmitted and received sound waves.

The hardware necessary for a low-cost, portable CW Doppler system is described in [45, 46]. In the system purposed by Molina et al., the signal from the receiving crystal is demodulated in quadrature and is sampled by a PC sound card. The Doppler signal is reproduced using the computer's speakers (i.e. to aid in probe placement), and a real-time sonogram is plotted on the screen [45, 46]. The original system was designed for the purposes of dialysis access monitoring. A similar system is currently being designed and tested by F. Livingston for the purposes of monitoring blood velocity in the femoral artery and vein.

6.1.2 Temperature Monitoring

Skin temperature is also known to vary with blood flow, and may be used to provide supplemental information [4]. As blood flow to an area is decreased, the skin grows cooler to the touch. This change in temperature could easily be measured using a thermistor (i.e. Surface Mount End-Banded Chip Thermistors, U.S. Sensor Corp.). Caution must be taken when incorporating this information into the pressure control algorithm, however, as temperature changes are usually considered to be a first order (or greater) response. This means that changes in temperature are not directly correlated with changes in blood flow (i.e. there is a lag).

6.1.3 Perfusion Monitoring

In addition to temperature, it may also be helpful to monitor muscle and subcutaneous tissue oxygenation levels in order to ensure that adequate perfusion is being achieved. Blood flow to the lower leg may become compromised with increasing pressure. Although safety stops limiting pressure to 50 mmHg or less will be incorporated, some patients may not be able to tolerate this level of compression. Additionally, patients suffering from severe arterial insufficiency may experience

arterial reflux even at low levels of applied pressure. While compression stockings are not prescribed in these cases, less severe arterial disorders may go undetected. If perfusion drops too low, healing time will be compromised and, in extreme cases, tissue death may result.

Oxygenation levels can be measured non-invasively using NIR technology. Briefly, oxygen is transported throughout the body bound to hemoglobin, and released when it reaches its destination site (i.e. muscles, tissues, etc.). By monitoring concentrations of bound (i.e. oxyhemglobin) and unbound (i.e. deoxyhemoglobin) hemoglobin, oxygenation levels can be determined:

$$\%Oxygenation = \frac{Oxyhemoglobin}{Oxyhemoglobin + Deoxyhemoglobin}$$

Oxyhemoglobin and deoxyhemoglobin are characterized by different absorption spectra in the near-infrared region (i.e. absorption for these species is maximized at 660 nm and 940 nm respectively). Due to the increasing demand for small, non-invasive medical devices, 660 nm and 940 nm are now being packaged and sold together (i.e. the L660/940-04A available from the Marubeni Corporation). Absorption is monitored using a photodetector, which again can be made small and low-profile.

6.1.4 Electronic Textiles

Actuation could some day be achieved using electroactive polymers (EAPs), a form of electronic textile. These organic materials change shape in response to an electrical stimulus. EAPs can be printed, sewn, knitted, or woven directly into the fabric to produce a lightweight, low-profile means of actuation [47]. Electronic textiles are advantageous insofar as they are more durable, flexible, and potentially easier to control than their pneumatic counterparts. Additionally, as EAPs are voltage-driven, they can be powered directly from a voltage source (i.e. they require fewer components).

"EAPs can be classified in two major categories: ionic EAPs (activated by an electrically-induced diffusion of ions or molecules) and electronic EAPs (activated by an external electric field and by Coulombian forces)" [47]. Electronic EAPs are characterized by a faster response time and are more efficient and reliable compared to ionic EAPs [47]. On the other hand, ionic EAPs may be better suited for battery-driven applications because they typically require lower voltages (on the order of 1 V), whereas electronic EAPs command higher voltages (i.e. 10-100 V/μm) [47]. Fortunately, high cycling speeds are not needed for intelligently-controlled compression stockings, rendering ionic EAPs more appropriate for this product.

Despite these seemingly positive attributes, electronic textile technology is still in its beginning stages. Many problems must be solved before widespread use can occur. For example, ionic EAPs exhibit poor mechanical properties (i.e. low active strain and high active stress), and lifetime is still a limiting factor. As previously mentioned, electronic EAPs require high driving voltages, and many are not suitable for macroscopic applications. Solutions to these problems are currently being investigated, leading to the possibility of using electronically actuated textiles in the future [47].

6.1.5 Other Medical-Grade Compression Stockings

The system described in this thesis was specifically designed for knee-length stockings, which are commonly used in the treatment of venous leg ulcers. The system could, however, easily be modified for use with thigh-length and anti-embolism product. Thigh-length stockings differ from knee-length stockings insofar as they are comprised of five compression zones– ankle, calf, popliteal, lower thigh, and mid-thigh. Dynamic regulation of all zones could again be accomplished using separate supply and exhaust valves for each zone. If necessary, two sensing systems could be used for the upper and lower leg. By expanding the use of intelligent, closed-loop control for the dynamic regulation of all medical-grade compression stockings, one could hope to treat a myriad of vascular conditions with only a few different products. This should serve to drive down the cost of compression stockings and improve the prescription process by limiting the number of decisions that the physician must make.

6.2 Summary

Venous leg ulcers remain a problem in the U.S., costing the health care industry upwards of $1 billion each year. A major portion of the cost is incurred as a result of prolonged healing time [1]. Compression therapy delivered in the form of bandages, stockings, or IPC devices is considered to be the cornerstone of the treatment process. Although studies have shown that this form of therapy shortens healing time by 40-80%, problems with patient compliance, improperly-fitted bandages/stockings, and/or a lack of portability reduces efficiency [8].

In an attempt to solve the problems associated with current compression therapy modalities, a dynamically-regulated compression stocking has been proposed by engineers at the Center for Robotics and Intelligent Machines and the Carolon Company. This would allow for individualized treatment using a generic stocking. To date, no such system exists. The envisioned stocking

would consist of three modules– a low-compression under-stocking, a pneumatically-controlled over-stocking, and a sensing system. Feedback from the sensing system would serve as an input to an intelligent control algorithm, which determines the appropriate level of pressure to be delivered. This serves to customize treatment, allowing for the potential exploration of different pressure profiles. Additionally, the problem of ill-fitting stockings would be rendered obsolete, and elderly/arthritic patients would no longer have difficulty donning compression hosiery.

This thesis explored the requirements for a robust, portable, sensing system that was capable of accurately reflecting the performance of the compression stocking. A novel means by which to measure blood flow velocity was investigated in Chapter 4. This system used an acoustic array to monitor blood flow. By measuring the time delay between the peaks of the pressure wave, blood velocity could be ascertained. Unfortunately, this technique failed both in terms of robustness and its ability to reflect venous blood flow conditions. The use of bio-impedance analysis for the purposes of quantifying the state of edema was discussed in Chapter 5. This technique has previously been used in both portable applications [48] and for quantifying edema [4], although the two concepts have never been integrated into one system. The system developed in this thesis was able to accurately measure small changes in lower leg volume resulting from artificially-induced swelling. Additionally, the system was found to be highly linear and predictable over the expected range of lower-leg impedance.

Upon discovery of a more accurate and robust means by measuring blood flow velocity, the sensing system will need to be tested by people with a variety of vascular conditions. Initially, data could be gathered by tracking changes in blood flow and swelling under manually controlled pressure application (i.e. by using different stockings and/or manual inflation of a pump). This data could then be processed by a neural network or some other form of machine learning algorithm in order to train a controller to regulate pressure with respect to optimizing blood flow and reducing swelling. In parallel to this effort, additional sensors (i.e. temperature and perfusion) could be tested in order to provide the controller with additional information. The use of electronic textiles could also be explored in order to achieve more lightweight and low-profile means of actuation. Upon successful implementation of this technology with knee-length stockings, the market could be expanded to include all medical-grade compression stockings, thus benefiting the maximum number of people.

References

[1] Jeffery W. Olin, Kathleen M. Beusterien, Mary Beth Childs, Caroline Seavey, Linda McHugh, and Robert I. Griffiths. Medical costs of treating venous stasis ulcers: Evidence from a retrospective cohort study. *Vascular Medicine*, 4:1–7, 1999.

[2] Tania J. Phillips. Successful methods for treating leg ulcers. *Postgraduate Medicine*, 105, 1999.

[3] Paula J. Stewart. The garments we wear. *LymphLink*, 19, 2007.

[4] H. Harry Asada and Melissa Barbagelata. Monitoring and treatment of leg edema and venous return disorder using bio-impedance sensors and a powered chair. Progress Report.

[5] O. Agu, G. Hamilton, and D. Baker. Graduated compression stockings in the prevention of venous thromboembolism. *British Journal of Surgery*, 86:992–1004, 1999.

[6] Simon J. Palfreyman, Rona Lochiel, and Jonathan A. Michaels. A systematic review of compression therapy for venous leg ulcers. *Vascular Medicine*, 3:301–313, 1998.

[7] H. A. Martino Neumann. Compression therapy with medical elastic stockings for venous diseases. *Dermatologic Surgery*, 24:765–770, 1998.

[8] M. Junger and H. M. Hafner. Interface pressure under a ready made compression stocking developed for the treatment of venous ulcers over a period of six weeks. *VASA*, 32:87–90, 2003.

[9] Jurg Hafner, Walter Luthi, Holger Hanssle, Gerhard Kammerlander, and Gunter Burg. Instruction of compression therapy by means of interface pressure measurement. *Dermatologic Surgery*, 26:481–487, 2000.

[10] K. G. Burnand and G. T. Layer. Graduated elastic stockings. *British Medical Journal*, 293:225–225, 1986.

[11] A. A. Ramelet. Compression therapy. *Dermatologic Surgery*, 28:6–10, 2002.

[12] Obi Agu, Daryll Baker, and Alexander M. Seifalian. Effect of graduated compression stockings on limb oxygenation and venous function during exercise in patients with venous insufficiency. *Vascular*, 12:69–76, 2004.

[13] R. Mani, K. Vowden, and E. A. Nelson. Intermittent pneumatic compression for treating venous leg ulcers. *Cochrane Database of Systematic Reviews*, 4:1–10, 2001.

[14] Jeffery Rowland. Intermittent pump versus compression bandages in the treatment of venous leg ulcers. *Australia and New Zealand Journal of Surgery*, 70:110–113, 2000.

[15] Philip Coleridge Smith, Sanjeev Sarin, James Hasty, and John H. Scurr. Sequential gradient pneumatic compression enhances venous ulcer healing: A randomized trial. *Surgery*, 108:871–875, 1990.

[16] Bernard Sigel, Annette L. Edelstein, Lane Savitch, James H. Hasty, and W. Robert Felix. Type of compression for reducing venous stasis: A study of lower extremities during inactive recumbency. *Archieves of Surgery*, 110:171–175, 1975.

[17] A. J. van Geest, J. C. J. M. Veraart, P. Nelemans, and H. A. M. Neumann. The effect of medical elastic compression stockings with different slope values on edema. *Dermatologic Surgery*, 26:244–247, 2000.

[18] Joep C. J. M. Veraart, Gerard Pronk, and H. A. Martino Neumann. Pressure differences of elastic compression stockings at the ankle region. *Dermatologic Surgery*, 23:939–939, 1997.

[19] E. Wintermantel. Microvascular auscultation: A new technique, using a diplo-microphone, for analysis of blood flow at suture lines in small arteries. *Acta Neurochirurgica*, 53:25–37, 1980.

[20] Wade D. Peterson, David A. Skramsted, and Daniel E. Glumac. Phoenix ambulatory blood pressure monitor project; Sub-project: Piezo flim pulse sensor. IEEE Phoenix Project, September 2005.

[21] C. J. Hartley and J. S. Cole. An ultrasonic pulsed doppler system for measuring blood flow in small vessels. *Journal of Applied Physiology*, 37:626–629, 1974.

[22] Lorie R. Pelc, Norbert J. Pelc, Stephen C. Rayhill, Luis J. Castro, Gary H. Glover, Robert J. Herfkens, D. Craig Miller, and R. Brooke Jeffrey. Arterial and venous blood flow: Noninvasive quantitation with MR imaging. *Radiology*, 185:809–812, 1992.

[23] Zhongping Chen, Thomas E. Milner, Shyam Srinivas, Xiaojun Wang, Arah Malekafzali, Martin J. C. van Gemert, and J. Stuart Nelson. Noninvasive imaging of in vivo blood flow velocity using optical doppler tomography. *Optics Letters*, 22:1119–1121, 1997.

[24] Peck Y. S. Cheang and Peter R. Smith. An overview of non-contact photoplethysmography. *Electronic Systems and Control Division Research*, pages 57–59, 2003.

[25] Frederick A. Jr. Anderson. Impedance plethysmography in the diagnosis of arterial and venous disease. *Annals of Biomedical Engineering*, 12:79–102, 1984.

[26] Robert Willeput, Christian Rondeux, and Andre de Troyer. Breathing affects venous return from legs in humans. *Journal of Applied Physiology*, 57:971–976, 1984.

[27] Nurhan Seyahi, Arzu Kahveci, Mehmet R. Altiparmak, Kamil Serdengecti, and Ekrem Erek. Ultrasound imaging findings of femoral veins in patients with renal failure and its impact on vascular access. *Nephrology Dialysis Transplantation*, 20:1864–1867, 2005.

[28] P. Hughes, C. Scott, and A. Bodenham. Ultrasonography of the femoral vessels in the groin: Implications for vascular access. *Anaesthesia*, 55:1192–1212, 2000.

[29] Steven L. Orebaugh. The femoral nerve and its relationship to the lateral circumflex femoral artery. *Anesthesia Analgesia*, 102:1859–1862, 2006.

[30] Irina Y. Petrova, Rinat O. Esenaliev, Yuriy Y. Petrov, Hans-Peter F. Brecht, Christer H. Svensen, Joel Olsson, Donald J. Deyo, and Donald S. Prough. Optoacoustic monitoring of blood hemoglobin concentration: A pilot clinical study. *Optics Letters*, 30:1677–1679, 2005.

[31] Lewis A. Eisen, Taro Minami, Hiroshi Sekiguchi, Jeffrey S. Berger, Paul Mayo, and Mangala Narasimhan. Ultrasound demonstration of asymmetry between the left and right femoral and radial arteries. *Chest*, 4:201S, 2006.

[32] O. Eiken and R. Kolegard. Comparison of vascular distensibility in the upper and lower extremity. *Acta Physiologica Scandinavica*, 181:281–287, 2004.

[33] Antoni Ivorra. Bioimpedance monitoring for physicians: An overview. Centre Nacional de Microelectronica: Biomedical Applications Group, July 2003.

[34] A. McEwan, G. Cusick, and D. S. Holder. A review of errors in multi-frequency EIT instrumentation. *Physiological Measurement*, 28:S197–S215, 2007.

[35] D. K. Swanson and J. G. Webster. Errors in four-electrode impedance plethysmography. *Medical and Biological Engineering and Computing*, 21:674–680, 1983.

[36] Alan Li and Jeritt Kent. Small current forms programmable 4- to 20-mA transmitter. *Electronic Design News*, pages 92–96, 2003.

[37] Kuo-Sheng Cheng, Cheng-Yu Chen, Min-Wei Huang, and Chien-Hung Chen. A multi-frequency current source for bioimpedance application. In *Information Technology Applications in Biomedicine (ITAB)*, 2006.

[38] Alexander S. Ross, G. J. Saulnier, J. C. Newell, and D. Isaacson. Current source design for electrical impedance tomography. *Physiological Measurement*, 24:509–516, 2003.

[39] APEX Microtechnology Corporation. Voltage to current conversion: Power operational amplifiers. Application Note 13.

[40] Rudolph Liedtke. Principles of bioelectrical impedance analysis. Website: www.rjlsystems.com, April 1997.

[41] A. Seo, M. Rys, and S. Konz. Measuring lower leg swelling: Optimum frequency for impedance method. *Medical & Biological Engineering & Computing*, 39:185–189, 2001.

[42] Akihiko Seo, Yuji Kondo, and Fumitaka Yoshinaga. A portable apparatus for monitoring leg swelling by bioelectrical impedance measurement. *Journal of Occupational Health*, 39:150–151, 1997.

[43] G. K. Belanger, M. L. Bolbjerg, N. H. H. Heegaard, A. Wiik, T. V. Schroeder, and N. H. Secher. Lower leg electrical impedance after distal bypass surgery. *Clinical Physiology*, 18:35–40, 1998.

[44] Y. Yamamoto, T. Yamamoto, and P. A. Oberg. Impedance plethysmography in human limbs: Part 1- on electrodes and electrode geometry. *Medical & Bilogicial Engineering & Computing*, 29:419–424, 1991.

[45] P. S. C. Molina, J. F. R. Baggio, and E. A. Togon. A low cost doppler system for vascular dialysis access surveillance. In *Proceedings of the 26th Annual International Conference of the IEEE EMBS*, 2004.

[46] P. S. C. Molina, J. F. R. Baggio, and E. A. Togon. Continuous wave doppler methods to dialysis access monitoring. In *Proceedings of the 26th Annual International Conference of the IEEE EMBS*, 2004.

[47] Federico Carpi and Danilo De Rossi. Electroactive polymer based devices for e-textiles in biomedicine. *IEEE Transactions on Information Technology in Biomedicine*, 9:295–318, 2005.

[48] Timo Vuorela, Kari Kukkonen, Jaana Rantanen, Tiina Jarvinen, and Jukka Vanhala. Bioimpedance measurement system for smart clothing. In *Proceedings of the Seventh IEEE International Symposium on Wearable Computers (ISWC'03)*, 2003.

Appendices

Appendix A

Specifications for Acoustic Blood Flow Monitoring System

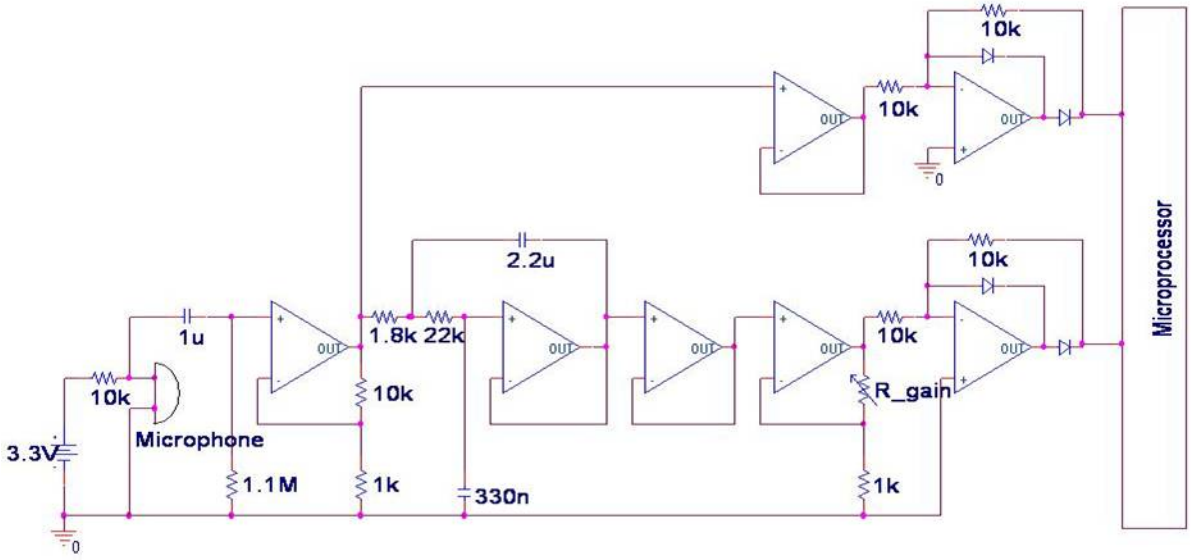

Figure A.1: Acoustic Blood Flow Monitoring System Schematic

Table A.1: Components for Acoustic Blood Flow Monitoring System

Component	**Part Number, Vendor**	**Qty**
Microphone	WM-52BM, Panasonic	1
Microprocessor	MSP430F149, Texas Instruments	1
Op-Amp	TLC2272, Texas Instruments	7
Small Signal Diodes	–	4
1.0K Resistor	–	2
1.8K Resistor	–	1
10K Resistor	–	6
22K Resistor	–	1
1.1M Resistor	–	1
R_{gain} Resistor	–	1
330n Capacitor	–	1
1.0u Capacitor	–	1
2.2u Capacitor	–	1

Gain Setting:

The overall amplification provided by the circuit (Figure .1) is the product of the the fixed initial amplification (i.e. 11x) and the variable final amplification:

$$Amplification = 11 * (1 + \frac{R_{gain}}{1.0K})$$

In order to achieve a final amplification of 1x, the appropriate amplifier and associated resistors can be eliminated from the circuit. Please refer to Figure .2 for further clarification.

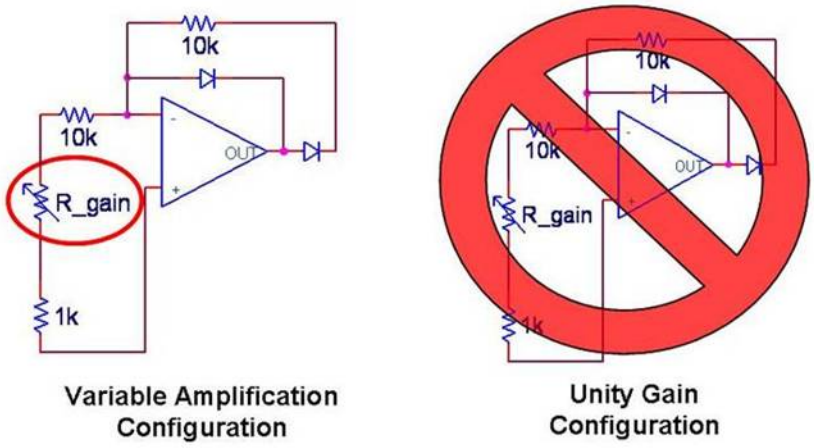

Figure A.2: Final Stage Amplification Options

Appendix B

Specifications for Edema Monitoring System

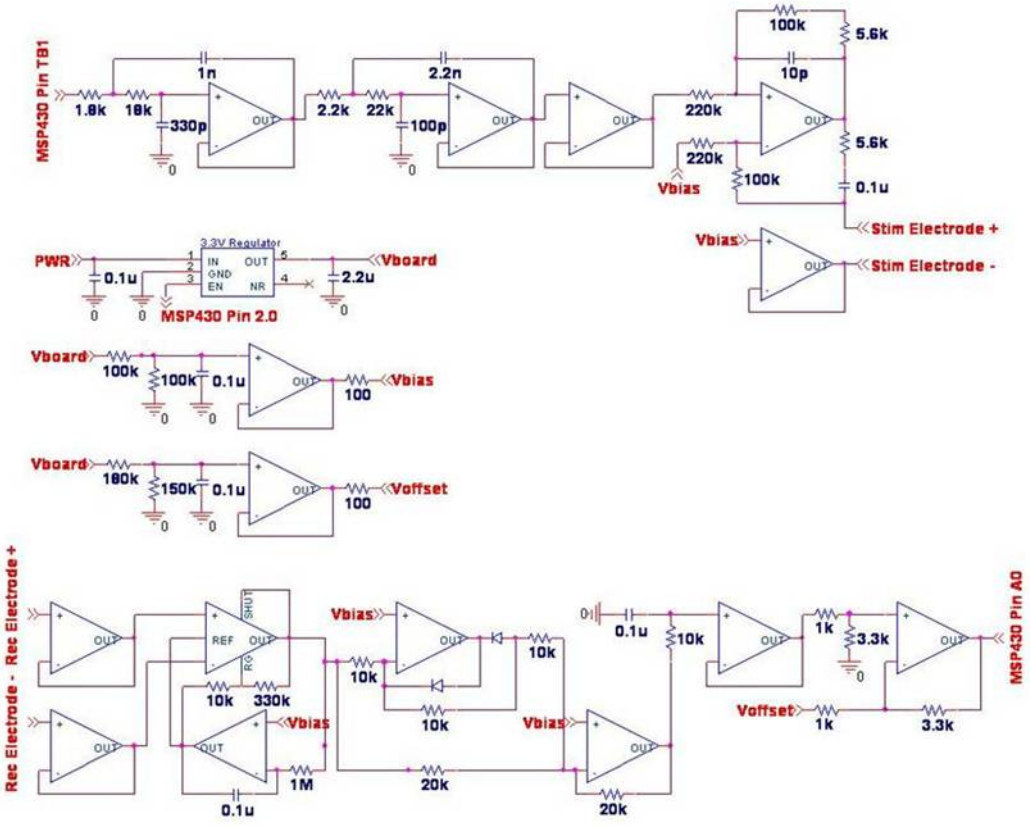

Figure B.1: Edema Monitoring System Schematic

Table B.1: Components for Edema Monitoring System

Component	**Part Number, Vendor**	**Qty**
3.3 V Regulator	TPS79933, Texas Instruments	1
Microprocessor	MSP430F149, Texas Instruments	1
32.768 kHz Oscillator	FX135A-327, Fox Electronics	1
Op-Amp	FAN4274, Fairchild Semiconductor	7
Instrumentation Amplifier	INA332, Texas Instruments	1
High-Speed Diode	BAW62, Philips Semiconductor	2
1M Resistor	–	1
1K Resistor	–	2
3.3K Resistor	–	2
20K Resistor	–	2
330K Resistor	–	1
5.6K Resistor (0.1%)	–	2
220K Resistor (0.1%)	–	2
22K Resistor	–	1
2.2K Resistor	–	1
18K Resistor	–	1
1.8K Resistor	–	1
180K Resistor	–	1
150K Resistor	–	2
100Ω Resistor	–	2
100K Resistor (0.1%)	–	2
100K Resistor	–	3
10p Capacitor	–	1
100p Capacitor	–	1
1n Capacitor	–	1
0.1u Capacitor	–	14
2.2u Capacitor	–	1

Safety Analysis (refer to IEC 2007 60601-1 Guideline):

The maximum injected current must not exceed *100 uA x f* for frequencies above 1 kHz, where f is the frequency of operation in kHz and the RMS value of current is measured) [34]. This means that for a 50 kHz signal, a maximum current of 5 mA RMS is permitted. The Edema Monitoring System limits the maximum injected current to 95 μA RMS (safety factor of 5.26x).

Appendix C

Specifications for 5-Channel USB Data Acquisition System

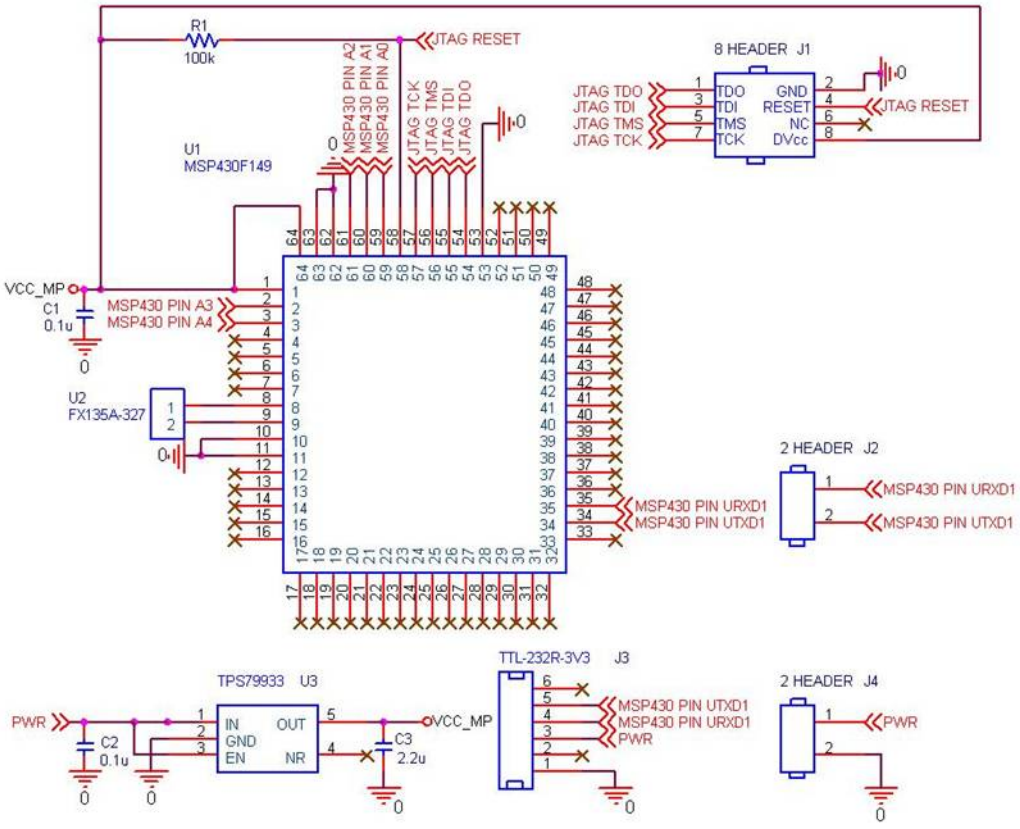

Figure C.1: Data Acquisition System Using MSP430F149 (Texas Instruments)

Table C.1: Components for Data Acquisition System

Component	Part Number; Vendor	Qty
Microprocessor	MSP430F149, Texas Instruments	1
MSP430 Parallel Port Debugging Interface	MSP-FET430PIF, Texas Instruments	1
8-Conductor Adapter for 14-Conductor Target Cable	–	1
USB to TTL Serial Converter Cable	TTL-232R-3V3, FTDI Chip	1
8-pin Header	–	1
2-pin Header	–	2
32.768 kHz Crystal Oscillator	FX135A-327, Fox Electronics	1
3.3 V Regulator	TPS79933, Texas Instruments	1
100K Resistor	–	1
0.1u Capacitor	–	2
2.2u Capacitor	–	1

**The 14-conductor target cable provided with the MSP-FET430PIF package may be used if the 8-pin header is replaced with a 14-pin header (pin-out is specified in manufacturer's data sheet).*

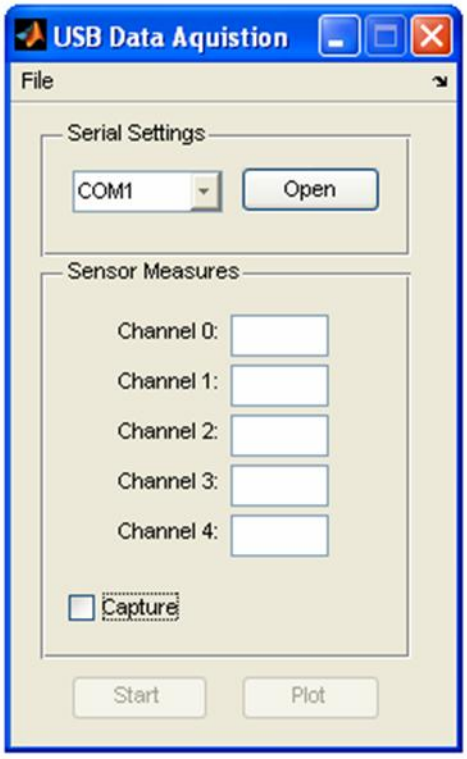

Figure C.2: GUI Screenshot (MATLAB code is provided in supplemental CD)